Molecular drivers of insecticide resistance in the Sahelo-Sudanian populations of a major malaria vector

Sulaiman S. Ibrahim[1, 2, 3, *], Abdullahi Muhammad[1, 4], Jack Hearn [1], Gareth D. Weedall [5], Sanjay C. Nagi [1], Muhammad M. Mukhtar [2], Amen N. Fadel[3], Leon M. J. Mugenzi[3], Edward I. Patterson[6], Helen Irving[1] and Charles S. Wondji [1,3]

[1] Vector Biology Department, Liverpool School of Tropical Medicine (LSTM), L3 5QA, UK

[2] Department of Biochemistry, Bayero University, PMB 3011, Kano, Nigeria

[3] LSTM Research Unit, Centre for Research in Infectious Diseases (CRID), P.O. Box 13591, Yaoundé, Cameroon

[4] Centre for Biotechnology Research, Bayero University, PMB 3011, Kano, Nigeria

[5] School of Biological and Environmental Sciences, Liverpool John Moores University, Liverpool L3 3AF, UK

[6] Department of Biological Sciences, Brock University, St. Catharines, Ontario, L2S 3A1, Canada.

* Correspondence: suleiman.ibrahim@lstmed.ac.uk ; Tel.: +44-74-4044-3871; ORCID: 0000-0003-0744-802X

Authors email addresses

Sulaiman S. Ibrahim: suleiman.ibrahim@lstmed.ac.uk

Abdullahi Muhammad: abdullahi.muhammad@lstmed.ac.uk

Jack Hearn: jack.hearn@lstmed.ac.uk

Gareth D. Weedall: g.d.weedall@ljmu.ac.uk

Sanjay C. Nagi: sanjay.nagi@lstmed.ac.uk

Muhammad M. Mukhtar: muhammadmahemukhtar@gmail.com

Amen N. Fadel: amen.fadel@crid-cam.net

Leon M. J. Mugenzi: leon.mugenzi@crid-cam.net

Edward I. Patterson: ipatterson@brocku.ca

Helen Irving: helen.irving@lstmed.ac.uk

Charles S. Wondji: charles.wondji@lstmed.ac.uk

Abstract

Information on common markers of metabolic resistance in malaria vectors from countries/regions sharing similar eco-climatic characteristics can facilitate coordination of malaria control. Here, we characterized populations of the major malaria vector *Anopheles coluzzii* from Sahelo-Sudanian region, spanning four sub-Saharan African countries, Nigeria, Niger, Chad and Cameroon. Genome-wide transcriptional analysis identified major genes previously implicated in pyrethroid and/or cross resistance to other insecticides, overexpressed across the Sahel. These include CYP450s, glutathione S-transferases, carboxylesterases, and cuticular proteins. Several variants identified recently as markers of resistance were found in high frequencies, including in the voltage-gated sodium channel (V402L, I940T, L995F, I1527T and N1570Y), the *acetylcholinesterase*-1 gene (G280S) and the *CYP4J5*-L43F. High frequencies of the phenotypically important chromosomal inversions, 2La, 2Rb and 2Rc were observed, with 2La alternative arrangement fixed across the Sahel, and some of the most commonly overexpressed metabolic resistance genes sitting in these inversions. Two most commonly overexpressed genes, *GSTe2* and *CYP6Z2* were functionally validated. Transgenic *Drosophila melanogaster* expressing *GSTe2* exhibited extremely high DDT and permethrin resistance (mortalities < 10% in 24 h). Serial deletion of the 5′ intergenic region, to identify putative nucleotide(s) associated with *GSTe2* overexpression, revealed that simultaneous insertion of adenine nucleotide and a transition (T->C), between Fork-head box L1 and c-EST putative binding sites are responsible for the high overexpression of *GSTe2* in the resistant mosquitoes. Transgenic flies expressing *CYP6Z2* exhibited marginal resistance towards 3-phenoxybenzyl alcohol and α-cypermethrin. However, significantly higher mortalities were obtained in *CYP6Z2* transgenic flies compared with controls, on exposure to the neonicotinoid, clothianidin. This suggests a possible bioactivation of clothianidin into a toxic intermediate, making it an ideal insecticide against populations of *An. coluzzii* overexpressing *CYP6Z2*. These findings will facilitate regional collaborations within the Sahel region, and refine implementation strategies through refocussing interventions, improving evidence-based, cross-border policy towards local and regional malaria pre-elimination.

Keywords: *Anopheles coluzzii*, Sahel, insecticides, pyrethroid, DDT, metabolic, resistance, genes, inversions.

Background

Since the year 2000 the massive scale-up in vector control interventions and treatment with antimalarial drugs had cut malaria incidence by ~40 % across Africa (Bhatt et al., 2015). Bolstered by this progress the World Health Organization (WHO) has been pushing to eliminate malaria, as proposed in the Global Technical Strategy (GTS) 2016-2030 (WHO, 2015). Unfortunately, the GTS, an ambitious framework with targets to reduce global malaria burden by 90 % in 15 years was dealt an immediate blow by a rebound in malaria transmission, with increased cases between 2016 and 2019 (WHO, 2018b, WHO, 2021). This stark warning of the risk posed to control and elimination efforts was a reflection of the lack of significant progress in the primary regions of interest in sub-Saharan Africa, which constitute 96 % of the 627,000 malaria-related deaths in 2020 alone (WHO, 2019, WHO, 2021). Indeed, as the WHO widens the net of malaria elimination (E-2025) its important to acknowledge that no meaningful progress will be made without progress in sub-Saharan Africa, where none of the six countries having the highest global burden of malaria (e.g. Nigeria alone contributing ~27 % of all cases) is on the path to elimination (WHO, 2018a).

The recent escalation of insecticide resistance in the major malaria vectors (Ibrahim et al., 2019b, Riveron et al., 2019, Toe et al., 2015) makes the development of molecular tools to anticipate emergence and predict spread of resistance across the African continent imperative, in order to achieve malaria control and elimination. For decades no simple molecular assays were available to track metabolic resistance and assess its impact on malaria control and transmission, until the recent discovery of two DNA markers in the *cis*-regulatory region of two cytochrome P450s, *CYP6P9a* (Weedall et al., 2019) and *CYP6P9b* (Mugenzi et al., 2019) in the major malaria vector *Anopheles funestus*; findings which allowed the design of simple PCR assays to detect and track metabolic resistance in the field. Unfortunately, these markers explain resistance only in southern Africa for *An. funestus*, since genetic basis of pyrethroid resistance, and cross-resistance with other insecticides is complex in other African regions with different fronts, driven by distinct genes in the presence of barriers to gene flow (Barnes et al., 2017, Weedall et al., 2019, Weedall et al., 2020). No major metabolic resistance markers for P450s and/or GSTs, functionally validated exist for the major malaria vectors of the *Anopheles gambiae* Complex, though it is the omnipresent vector species with widespread

108 presence across Africa (Bruce-Chwatt, 1951). This is hindering early detection and tracking of
109 molecular drivers of resistance in this species, slowing down optimal evidence-based control
110 measures and resistance management.

111 Major genomic regions associated with metabolic resistance to pyrethroids in *An. gambiae*
112 sensu lato include the *CYP6* P450 clusters on the 2R and 3R chromosomes, and a *GST* epsilon
113 (*GSTe*) cluster on chromosome 3R (Anopheles gambiae Genomes et al., 2017), with some key
114 resistance-associated genes functionally validated. These genes include *CYP6P3* shown to
115 confer cross resistance to pyrethroids and organophosphates (Muller et al., 2008, Yunta et al.,
116 2019), *CYP6M2* conferring cross resistance to pyrethroids (Stevenson et al., 2011, Mitchell et
117 al., 2012b) and DDT (Mitchell et al., 2012b), as well as *GSTe2* shown to confer resistance to
118 DDT (Mitchell et al., 2014). For *GSTe2*, in addition to the I114T marker (Mitchell et al., 2014),
119 a recent study has found a novel mutation (*Gste2*-119V) associated with resistance (Lucas et
120 al., 2019) using a high-throughput genotypic panel for markers. Functional validation is
121 required establish the empirical evidence of the role of this mutation in resistance. What has
122 been missing in the case of *Anopheles gambiae/coluzzii* is reliable molecular markers of
123 resistance for major metabolic gene families, e.g. P450s (with field and laboratory validated
124 data) to aid creation of DNA-based diagnostic assays which will allow (i) easy tracking of
125 resistance in the field (e.g. the case of 119F-*GSTe2* mutation in *An. funestus* (Riveron et al.,
126 2014b), and (ii) determination of the operational impact of the resistance markers in the field,
127 as recently done for 119F-*GSTe2* (Menze et al., 2020) and *CYP6P9a*_R/*CYP6P9b*_R markers
128 (Mugenzi et al., 2019, Weedall et al., 2019) in *An. funestus*.

129 The *An. gambiae s.l.*, especially populations in the semi-arid steppe, exhibit high frequency of
130 paracentric chromosomal inversions [one of the most effective instruments for speciation and
131 local adaptations (Ayala et al., 2014, Dobzhansky, 1971, Kirkpatrick, 2010)], maintained in
132 spatially and temporally heterogenous environment, and which segregate along climatic
133 gradients of increasing aridity (Coluzzi et al., 1979)]. The 2L inversions are associated with
134 resistance to desiccation in adults (Fouet et al., 2012, Gray et al., 2009) and thermal stress in
135 larvae (Cassone et al., 2011). It was also shown that inversion 2La assorts with insecticide
136 resistance, e.g., dieldrin plus fipronil (Brooke et al., 2000), and is associated with
137 thermotolerance and permethrin resistance in the Sahelain *An. coluzzii* (Ibrahim et al., 2021).

138 To support malaria pre-elimination effort in sub-Saharan Africa we targeted the Sahelo-
139 Sudanian region, which represent northern-most limit of malaria endemicity in sub-Saharan
140 Africa, and where malaria is highly seasonal [offering excellent target for pre-elimination
141 effort through sustained seasonal vector control and seasonal malaria chemoprevention
142 (Cairns et al., 2012)]. Focusing on the predominant malaria vector, *An. coluzzii* from
143 Sudan/Sahel transects of four countries, Nigeria, Niger, Chad and Cameroon (Ibrahim et al.,
144 2019b, Ibrahim et al., 2019c, Fadel et al., 2019, Ibrahim et al., 2019a) we identified the major
145 metabolic resistance genes mediating pyrethroid resistance and cross-resistance in this region,
146 established the genetic variants which explained the resistance. We also functionally validated
147 the roles of two major candidate genes in the resistance (*CYP6Z2* and *GSTe2*), as well as single
148 nucleotide polymorphism in the 5′ regulatory elements of *GSTe2,* responsible for its
149 overexpression in the resistant population.

150

151 **Materials and Methods**

152 **Study Site and Mosquito Sampling**

153 Blood fed female *An. coluzzii* mosquitoes, resting indoor were collected at one locality each in
154 Sudan/Sahel (Figure S1): Hadiyau (HAD: 12°21′38″N, 9°59′15″E), a Sudan/sub-Sahel village in
155 northern Nigeria; Takatsaba (TAK: 13°44'01.8"N 7°59'05.2"E), a Sahel village in southern
156 Niger; Simatou (SIMAT: 10°50'40.7"N 14°56'40.9"E), a Sudan/sub-Sahel village in Maga
157 Department, far north of Cameroon; and Massakory (CHAD: 12° 6′ N, 15° 02′ E), a Sahel town
158 in Chad Republic. Details of sampling approaches and resistance profiles of mosquitoes
159 collected from Nigeria, Niger, and Chad are available in previously published articles
160 (Ibrahim et al., 2019b, Ibrahim et al., 2019c, Ibrahim et al., 2019a). As in the above countries
161 the Simatou F_1 females were also highly pyrethroid resistant, with a mortality of only 3.7%
162 from WHO tube bioassays using 0.05% deltamethrin, and no mortality at all with 0.75%
163 permethrin (data not published).

164

165

166 **Genome-wide transcriptional analysis for common insecticide resistance genes in the**
167 **Sahel/sub-Sahel regions**

168 ***RNA extraction, library preparation and sequencing***

169 The RNA was extracted using the Arcturus PicoPure RNA isolation Kit (Applied Biosystems,
170 CA, USA) from three pools of 8 F_1 *An. coluzzii* females (2-4 day old) alive after exposure to
171 deltamethrin (resistant, R), unexposed (control, C), and also from unexposed females of the
172 fully susceptible laboratory colony of *An. coluzzii*, Ngoussou (Mitchell et al., 2012a)
173 (susceptible, S). RNA isolation was carried out following the manufacturer's protocol with
174 *Dnase* I-treatment to remove contaminating DNA. The quantity and quality of RNA was
175 measured using a NanoDrop spectrophotometer (ThermoFisher, MA, USA) and Bioanalyzer
176 (Agilent, CA, USA).

177 Library preparation, sequencing and data quality control were carried out by the Centre for
178 Genomic Research (CGR), University of Liverpool, UK. RNA samples were subjected to
179 poly(A) mRNA enrichment and libraries prepared from the poly(A) mRNA-enriched
180 materials (dual-indexed, strand-specific RNAseq libraries were prepared using the NEBNext
181 polyA selection and Ultra Directional RNA library preparation kits). Libraries were
182 sequenced on a single lane of an Illumina HiSeq 4000 (paired-end, 2x150 bp sequencing,
183 generating data from >280 M clusters per lane). Basecalling and de-multiplexing of indexed
184 reads were performed by CASAVA version 1.8.2 (Illumina). De-multiplexed fastq files were
185 trimmed to remove Illumina adapter sequences using Cutadapt version 1.2.1 (Martin, 2011).
186 Option -O 3 was used, so that the 3' end of any reads which matched the adapter sequence for
187 3 bp or more were trimmed. Reads were further trimmed to remove low quality bases
188 using Sickle version 1.200 (Joshi and Fass, 2011) with a minimum window quality score of 20.
189 Reads shorter than 20 bp after trimming were removed. If both reads from a pair passed this
190 filter, each was included in either the R1 (forward reads) or R2 (reverse reads) file. If only one
191 of a read pair passed this filter, it is included in the R0 (unpaired) file. Statistics were generated
192 using fastq-stats from EAUtils (Aronesty, 2011). Summary of total number of reads for each
193 sample and distribution of trimmed read length for forward (R1) and reverse (R2) reads and
194 reads unpaired after trimming (R0) are provided in Figure S2.

195

196 ***Data analysis and estimation of transcript abundance by tag counting and differential gene***
197 ***expression***

198 Paired data for each replicate per country was aligned to the *An. gambiae* reference transcript
199 ome AgamP4.10 downloaded from VectorBase (https://vectorbase.org/) in salmon (0.11.4),
200 using 'validate mappings', 'seqBias', 'gcBias' and 'rangeFactorizationBins 4' flags. Read
201 mapping results (pre-alignment and post-alignment descriptive statistics (flagstat output
202 files) showing sequencing depth and coverage are given in Tables S1 and -S2, respectively.
203 Salmon results were converted into a gene expression matrix using the Bioconductor package
204 'tximport' for input to DESeq2 1.26.0 (Love, 2014). Differential gene expression was tested for
205 the three possible combinations of Exposed (R, deltamethrin resistant), Unexposed (C,
206 control) and Susceptible replicates (S). For results interpretation $\log_2$-fold change thresholds
207 of 1 was imposed, with false discovery rate adjusted p-values of 0.05 applied to accept
208 significance. Principal components analysis implemented in DESeq2 was used to examine
209 relationships between respective replicates and treatments. This was carried out based on the
210 500 most variable genes, with data transformation (normalisation/scaling) as implemented in
211 VST (DESeq2). For visualisation of expression results, volcano plots were created using the
212 Enhanced Volcano package (Blighe, 2018) using the top most overexpressed genes from lists
213 which were prepared with $\log_2$FC cut off of 1 and p value of 0.01. Heatmaps were generated
214 (Gu et al., 2016) using the list of the top 50 most overexpressed metabolic resistance genes
215 with $\log_2$FC cut off of 1 and p value of 0.01.

216

217 ***Gene Ontology Enrichment and Mapping/Functional annotations***

218 The enrichment analysis for GO terms was carried out using a topGO package (Alexa A., 2021)
219 against *An. gambiae* (AgamP4.10), with data reannotated using EggNOG v5.0
220 (http://eggnog5.embl.de/#/app/home). Gene lists used in topGO are from the $\log_2$FC = 0, p
221 <0.05 analysis (the default in DESeq2). For the data from each site (country) six set of results
222 were generated (R C and S contrasts) each for genes either up- or down-regulated in each
223 contrast, for molecular function (MF) and biological process (BP) ontologies. For analysis the
224 GO terms lists for MF were used as input into the Revigo (Supek et al., 2011) for interpretation

225 and visualisation, querying the Whole Uniprot database, and SimRel setting for semantic
226 similarity measurements.

227

228 **Quantitative PCR measurement of expression profiles of metabolic resistance genes**

229 The level of expression of 12 resistance-associated genes was validated by qRT-PCR using the
230 primers provided in Table S3. These include the *GSTe2* (AGAP009194) and *GSTZ1*
231 (AGAP002898), *CYP6Z2* (AGAP008218), *CYP6Z3* (AGAP008217), *CYP4C27* (AGAP009246),
232 *CYP4G16* (AGAP001076), *CYP4G17* (AGAP000877), *CYP6P3* (AGAP002865), *CYP6M2*
233 (AGAP008212), *CYP9K1* (AGAP000818), a *UGT-B19* (AGAP007920) and *COEBE3C*
234 (AGAP005372). The qRT-PCR was carried out using cDNA extracted from 1 μg of total RNA
235 from each of three biological replicates (and three technical replicates each) from the Resistant
236 (R), Control (C) and Ngoussou (S), for each of the four countries. Protocol followed was as
237 established in previous studies (Riveron et al., 2014a), with relative expression level and fold
238 change (FC) of each target gene in R and C relative to S calculated according to the 2^{-}
239 $^{\Delta\Delta CT}$ method incorporating the PCR efficiency (Schmittgen and Livak, 2008) after
240 normalization with the housekeeping genes ribosomal protein S7, *RPS7* (AGAP010592) and
241 glycerol-3-phosphate dehydrogenase (NAD+), *GPDH* (AGAP007593). Significant differences
242 were calculated using ANOVA with Dunnett's post hoc test.

243

244 ***Detection of Signatures of Selective Sweep***

245 To detect signature of select sweeps in the major metabolic resistance genes of interest, a
246 RNAseq population genetics pipeline, the Snakemake workflow
247 (https://zenodo.org/record/6078337) was utilised. F_{st} (Hudson et al., 1992) per gene between
248 population pairs and Tajima's D per gene within population were estimated after calling
249 genomic variants with *Freebayes*. This was performed against all SNPs passing quality and
250 missingness filters. Population branch statistic (PBS) scans may also be performed, conditional
251 on the presence of three suitable populations (Yi et al., 2010). It is also possible to run Hudson's
252 F_{st} and PBS scans, taking the average for each protein-coding gene, as opposed to in windows.
253 The population genetics statistical analyses are calculated in scikit-allel v1.2.1 (Alistair Miles,
254 2020).

255 ***Establishment of allele frequencies of variants in genes of interest***

256 After genome alignment, RNA-Seq-Pop utilises samtools (https://zenodo.org/record/6078337)
257 to cross check specific positions of the genome, calculating raw allele frequencies at those sites
258 with a custom R script.

259

260 ***Detection of chromosomal inversion polymorphisms and metabolic genes within its***
261 ***breakpoint***

262 A modified version of the Python 3 program, compkaryo (Love et al., 2019) was used to
263 karyoptype the major, phenotypically important inversion polymorphisms in chromosome 2,
264 and calculate its frequencies, *in silico*, using the previously identified tag SNPs significantly
265 associated with inversions. This allows to predict with high confidence genotypes of the six
266 common polymorphic inversions on chromosome 2 in individually sequenced genomes of the
267 field *An. coluzzii*, as well as in the Ngoussou. Compkaryo uses the Ag1000 database
268 (The *Anopheles gambiae* 1000 Genomes Consortium 2017) (Anopheles gambiae Genomes et al.,
269 2017) by leveraging a subset of cytologically karyotyped specimens to develop a
270 computational approach for karyotyping applicable to whole genome sequence.
271 Modifications in the Snakemake pipeline allows for variable ploidy (useful in the case of
272 replicates from our pooled RNAsequencing samples) here.

273

274 **Functional validation of the role of commonly overexpressed resistance-associated genes**

275 ***Comparative analysis of coding sequences of major resistance genes***

276 To establish presence of allelic variants which could impact catalytic activities, full length
277 coding sequences (cDNAs) of the two resistance-associated genes, *GSTe2* and *CYP6Z2* were
278 amplified and sequenced from alive mosquitoes in the four Sahel countries, as well as from
279 Ngoussou. This was done using total RNA extracted from 5 individual pools of 8 F_1 *An.*
280 *coluzzii* females (2-4 day old) alive after exposure to deltamethrin (resistant, R for *CYP6Z2*) or
281 DDT (R for *GSTe2*). Protocol for RNA extraction was as described in previous section, above.
282 Amplification was done using Phusion HotStart II Taq Polymerase (ThermoFisher
283 SCIENTIFIC, MA, USA) and the Full primers listed in Table S4. The PCR mix comprised 5X

284 Phusion HF Buffer (containing 1.5 mM $MgCl_2$), 85.7 µM deoxynucleotides (dNTPs), 0.34 µM
285 each of forward and reverse primers, 0.015 U of Phusion HotStart II DNA Polymerase
286 (Fermentas, MA, USA), 10.71 µL of ddH_20 and 1 µL cDNA. Thermocycling conditions were 1
287 cycle at 95 °C for 5 min; followed by 35 cycles each of 94 °C for 20 s, 60 °C for 30 s, 72 °C for 2
288 min (1 min for *GSTe2*); and finally, one cycle at 72 °C for 5 min. PCR products were cleaned
289 with a QIAquick® PCR Purification Kit (QIAGEN, Hilden, Germany) and ligated into the
290 pJET1.2/blunt cloning vector using the CloneJET PCR Cloning Kit (ThermoFisher
291 SCIENTIFIC, MA, USA). These were then cloned into *E. coli DH5α*, plasmids miniprepped
292 with the QIAprep® Spin Miniprep Kit (QIAGEN) and sequenced on both strands using
293 pJET1.2 primers.

294 Polymorphisms were detected through examination and manual editing of sequence traces
295 using BioEdit version 7.2.3.0 (Hall, 1999) and nucleotide differences in sequences aligned
296 using CLC Sequence Viewer 7.0 (http://www.clcbio.com/). Different haplotypes were
297 compared by constructing a phylogenetic maximum likelihood tree using MEGA X (Kumar
298 et al., 2018). Genetic parameters of polymorphism including number of haplotypes (h) and its
299 diversity (H_d), number of polymorphic sites (S) and nucleotide diversity (π) were computed
300 using DnaSP v6.12.03 (Rozas et al., 2017). The DNA sequences were deposited in GenBank,
301 with accession numbers: XXXXX-YYYYY.

302

303 ***Characterization of the 5′ regulatory regions of GSTe2 and CYP6Z2***

304 *Amplification, cloning and sequence characterisation of 5′ regulatory element*

305 To investigate presence of genetic variants in the regulatory elements, which could be
306 responsible for overexpression of *GSTe2*, 351 bp intergenic regions (spanning the 43 bp 3′ UTR
307 of *GSTe1*, 248 bp flanking sequence and 60 bp 5′UTR of *GSTe2*) preceding the start codon were
308 amplified from 10 each of DDT-alive and -dead females from the 4 Sahel countries, as well as
309 from the Ngoussou females (primers provided in Table S4). For *CYP6Z2*, a 1078 bp intergenic
310 region was retrieved from the VectorBase and used for amplification of the putative 5′-
311 regulatory elements. Primers spanning 38 bp 3′ UTR of *CYP6Z1*, a 937 bp flanking sequence
312 and 103 bp 5′UTR of *CYP6Z2*, preceding the start codon of *CYP6Z2* were used to amplify

313 fragments from 10 each of deltamethrin-alive and -dead females from Nigeria and Niger, as
314 well as from the Ngoussou females. Amplification was carried out using HotStart II
315 Polymerase (ThermoFisher SCIENTIFIC, MA, USA) with similar thermocycling conditions as
316 outlined above for coding region of *GSTe2* and *CYP6Z2,* respectively. Purification of PCR
317 amplicons, cloning into pJET1.2 vector, sequencing and polymorphism analysis were done as
318 outlined above. The DNA sequences were deposited in GenBank, with accession numbers:
319 XXXXX-YYYYY.

320 The 351 bp 5′-UTR fragments of *GSTe2* and 1078 bp fragment of the *CYP6Z2* were analysed
321 with the Gene Promoter Miner (http://gpminer.mbc.nctu.edu.tw/) and MatInspector
322 (Cartharius et al., 2005) to identify putative promoter elements, predict transcription start
323 (TSS) and potential transcription factor binding sites.

324

325 *Cloning of GSTe2 and CYP6Z2 5′ regulatory elements in PGL3-Basic vector and dual luciferase*
326 *reporter assay*

327 Following analysis of the above sequences the 351 bp intergenic fragments of *GSTe2* were
328 amplified from the most predominant sequences of DDT-alive, DDT-dead and Ngoussou.
329 Same was done for for *CYP6Z2* amplifying 1087 bp fragment from deltamethrin-alive and -
330 dead, and Ngoussou. Primers bearing *kpn*I and *BgL*II sites (Table S4) allowed incorporation
331 into pGL3-Basic reporter vector containing luciferase gene from the firefly *Photinus pyralis*
332 (Promega, Wisconsin, USA). Amplification was carried out using Phusion HotStart II
333 Polymerase, with conditions as above, followed by purification of PCR amplicons, and
334 cloning into pJET1.2 vector. Positive colonies (sequencing primers for pGL3-Basic provided
335 in Table S4) were miniprepped; the minipreps digested with the above restriction enzymes,
336 gel-purified and ligated upstream of luciferase gene in pGL3-Basic vector already linearized
337 with the same restriction enzymes. Positive colonies were cloned and miniprepped and
338 concentrations of the recombinant plasmids adjusted to 200 ng/μL before co-transfection.
339 Protocols for maintenance of the *An. gambiae* cell line 4a-3B (MRA-919,
340 https://www.beiresources.org/), co-transfection of 200 ng of either *GSTe2* or *CYP6Z2* promoter
341 constructs, LRIM promoter in pGL3-Basic vector (Lynd and Lycett, 2011), or promoter-less
342 pGL3-Basic control, with 1 ng/μL of internal control, sea pansy *Renilla reniformis* luciferase

343 containing the *Drosophila* Actin *5C* promoter in pRL-null (Lynd and Lycett, 2011), are provided
344 in File S1 (additional text for Methods and Results). Protocol for cell lysis and measurement
345 of the activities of the firefly luciferase (Dual-Luciferase Reporter Assay kit, Promega), with
346 normalisation using the Renilla luciferase activity, were as outlined in the Promega Quick
347 Protocol, and provided in detail in File S1.

348 Assay background was also measured using lysate from non-transfected control cells. Results
349 were compared using a two-tailed Chi-Square test of independence as implemented in
350 GraphPad Prism 7.02 (GraphPad Inc., La Jolla, CA, USA).

351

352 *Generation of GSTe2 promoter deletion constructs and assays*

353 The intergenic region separating *GSTe1* from *GSTe2* was progressively delineated. Partial
354 fragments of the 5′ regions (encompassing the 3′-UTR of *GSTe1*, the *GSTe1*/*GSTe2* flanking
355 region and the 5′-UTR of the *GSTe2*) were created by sequential deletion using forward
356 primers (provided in Table S4, with numbers in primer names denoting distance from the
357 AUG start codon of *GSTe2*). Reverse primers were those initially used for amplification of the
358 full 351 bp nucleotide fragments. These fragments include (i) 308 nucleotides fragment
359 generated from deletion of the 43 bp 3′-UTR of the *GSTe1* (-308 primers) obliterating cellular-
360 Myb (c-Myb) transcriptional factor binding site; (ii) 291 nucleotide fragments generated from
361 deletion of *GSTe1* 3′-UTR plus 38 nucleotides of the flanking region (-270 primers), which
362 removed in addition δ elongation factor 1 (δEF1) binding site; (iii) 262 nucleotide fragments
363 produced from deletion of *GSTe1* 3′-UTR plus 46 nucleotides of the flanking region (-262
364 primers), which obliterated in addition Forkhead box L1 (FOX-L1) putative binding site; as
365 well as (iv) 232 nucleotide fragments produced from deletion of *GSTe1* 3′-UTR plus 75
366 nucleotides of the flanking region (-232 primers), located 11 nucleotides from the c-EST
367 binding site/grainy head transcription factor binding site. Also, to assess the impact of
368 removing the 5′UTR of *GSTe2*, 43 nucleotides upstream the AUG codon were deleted (from
369 the 60 nucleotide 5′-UTR of both the Sahel-alive and Ngoussou), leaving the putative
370 transcription start site position motif untouched. This was done using the original forward
371 primer for the 351 nucleotides intergenic region, with a newly designed primer,
372 GSTe2_minus_5′-UTR-R (Table S4).

373 ***Characterisation of major resistance genes using transgenic analysis***

374 *Cloning and microinjection of GSTe2 and CYP6Z2 in Drosophila melanogaster flies*

375 Transgenic flies expressing recombinant GSTe2 and CYP6Z2 were generated using
376 GAL4/UAS system and used in contact bioassays to confirm if over-expression of these genes
377 alone can confer resistance to insecticides. Transgenic flies were produced out as outlined in
378 a previous publication (Ibrahim et al., 2015). Details of amplification of full-length *GSTe2* and
379 *CYP6Z2* from the predominant alleles of sequences of cDNA, cloning into pUASattB vector,
380 microinjection into germ-line *D. melanogaster* lines, crossing of the UAS-lines with the GAL4-
381 Actin driver strain are outlined in File S1.

382 To confirm overexpression of *GSTe2* and *CYP6Z2* in the transgenic flies three replicates each
383 of 6 females (both experimental and control group) were used for qRT-PCR using a previously
384 established protocol (Riveron et al., 2014a). Total RNA and cDNA were extracted as described
385 above, and the relative expression levels of the transgene were assessed by qRT-PCR, with
386 normalization using the *RPL11* housekeeping gene. The qtrg primers used for the two genes
387 and the *RPL11* primers are provided in Table S4.

388

389 **Insecticide Susceptibility Contact Bioassay**

390 For insecticide bioassays, 3- to 4-day old experimental and control F_1 females were exposed to
391 0.15 % deltamethrin, 2 % permethrin, 0.05 % α-cypermethrin, 4 % DDT and 2 % clothianidin-
392 impregnated papers prepared in acetone and Dow Corning 556 Silicone Fluid (BHD/Merck,
393 Hesse, Germany). Flies overexpressing *CYP6Z2* were also exposed to the primary product of
394 hydrolysis of pyrethroids: 4 % and 20 % (5x) 3-phenoxybenzaldehyde (PBAld) and 3-
395 phenoxybenzyl alcohol (PBAlc). Transgenic flies expressing *GSTe2* were exposed to 2 %
396 permethrin, 0.15 % deltamethrin, 0.05 % α-cypermethrin and 4 % DDT only. Impregnated
397 papers were rolled and introduced into 45 cc plastic vials to cover the entire wall and the vials
398 plugged with cotton soaked in 10 % sucrose (Riveron et al., 2014a). 20–25 flies were placed in
399 each vial, and the mortality plus knockdown scored at 1 h, 3 h, 6 h, 12 h and 24 h of exposure
400 to the insecticides. For each insecticide, assays were performed in 6 replicates and Student's

401 t-test used to compare the mortality plus knockdown between the experimental groups and
402 the control.

403

404 **Results**

405 **Genome-wide transcriptional profile of the Sahelian *An. coluzzii* populations**

406 A three-way pairwise comparison was conducted for the data from each country: resistant *vs*
407 susceptible (R-S), resistant *vs* unexposed control (R-C) and unexposed control *vs* susceptible
408 (C-S). This captures background variations due to geographical differences in the resistant vs
409 susceptible (R-S) comparison, accounts for genes overexpressed due to induction (R-C
410 comparison), as well as genes that are constitutively overexpressed (C-S comparison). A total
411 of 1384 genes were significantly differentially expressed (FDR-adjusted $p < 0.05$ and $\log_2$ fold
412 change threshold of $1/FC \geq 2$) in R-S comparison in Nigeria (1077 upregulated and 307 down-
413 regulated); 1185 genes were differentially expressed in C-S (1002 upregulated and 183
414 downregulated); and 295 genes in R-C (129 upregulated and 166 downregulated). Of these,
415 52 genes were commonly differentially expressed in all 3 comparisons (Figure S3, panel a),
416 including the upregulated genes, *COEAE80* (AGAP006700), *CYP4H18* (AGAP028019),
417 *CYP4H17* (AGAP008358) and cuticular proteins, *CPLCX3* (AGAP006149), *CPR59*
418 (AGAP006829), *CPR76* (AGAP009874) and *CPR75* (AGAP009871). The Figure S3, panels a-d
419 depicts the differentially expressed genes for the four countries. For Niger, 881 genes were
420 differentially expressed in R-S comparison (619 upregulated and 262 down-regulated) (Figure
421 S3b); 1256 genes were differentially expressed in C-S (986 upregulated and 270
422 downregulated); and 196 genes in R-C (81 upregulated and 115 downregulated). Of these, 22
423 genes were commonly differentially expressed in all 3 comparisons [including the
424 upregulated *aminopeptidase N1* (AGAP012757), *CYP6Z2* (AGAP008218), *chymotrypsin-3*
425 (AGAP006711) and *chymotrypsin-2* (AGAP006710), and an acid trehalase (AGAP008547)]. For
426 Chad, 1392 genes were differentially expressed in R-S comparison (975 upregulated and 417
427 down-regulated) (Figure S3c); 1284 in C-S (105 upregulated and 269 downregulated); and 526
428 genes in R-C (270 upregulated and 256 downregulated). Of these, 97 genes were commonly
429 differentially expressed in all 3 comparisons [including *CYP4C27* (AGAP009246), *SULTD1*
430 (AGAP012672), *aminopeptidase N1*, and diverse cuticular proteins, e.g. chitinase (*Cht24*,

431 AGAP006191, *CPFL1* (AGAP010902), *CPCFC1* (AGAP007980), *CPLCX3*, *CPR24*
432 (AGAP005999), *CPR106* (AGAP006095) and *CPR130* (AGAP000047). Finally, for Cameroon,
433 376 genes were differentially expressed in R-S comparison (204 upregulated and 172 down-
434 regulated) (Figure S3d); 932 in C-S (778 upregulated and 154 downregulated); and 116 genes
435 in R-C [only 9 upregulated and 107 downregulated (probably due to a single, low quality
436 replicate in the raw data from Cameroon (Figure S2). Not surprising, only 7 genes were
437 commonly differentially expressed in all 3 comparisons. These include the highly upregulated
438 gene, *GSTe2* (AGAP009194) and *chymotrypsin-1* (AGAP006709).

439 All data analysed together (Figure S3e) revealed no single gene differentially expressed in
440 common; possibly due to the low quality with the Chad unexposed (C) data. Analysis of data
441 from Nigeria, Niger and Chad, revealed a single gene (AGAP000046, transporter major
442 facilitator superfamily) differentially expressed across all countries (Figure S3f). Niger and
443 Chad shared *hexamerin* (AGAP010658), *aminopeptidase N1*, and unknown protein,
444 AGAP0290967; Nigeria and Niger share only a single gene, AGAP003248; while seven genes
445 were common to Nigeria and Chad, including *CPLCX3*.

446 Principal component analysis for the top 500 most variable genes in all experimental arms
447 revealed data from field samples (R and C) from all four countries clustering closer in PC1
448 and PC2 axes, away from the data from the susceptible females, Ngoussou (Figure S4).

449

450 *Analysis of the common differentially expressed genes across the Sahel*

451 The most differentially expressed genes were presented in Figure 1, a volcano plot of fold
452 change *vs* significance levels for Nigeria and Niger, and Figure 2, for Chad and Cameroon.
453 Exhaustive lits of these genes of interest is provided in File S2. Comparisons of genes
454 commonly, upregulated and/or downregulated in R-S/R-C/C-S, from the four countries
455 revealed similar transcriptomic profiles between R and C compared with the S. The most
456 commonly and consistently overexpressed genes across the Sahel (taking account mean
457 expressions) are the chymotrypsins, 3, -2 and -1 (*CHYM3*/AGAP006711 and
458 *CHYM2*/AGAP006710 and *CHYM1*/AGAP006709) (Figures 1 and 2, File S2), the glutathione
459 S-transferase, *GSTe2* (AGAP009194), an aquaporin, *AQP3* (AGAP010326), *CYP6Z2*

460 (AGAP008218), *CYP6Z3* (AGAP008217), *CYP4C27* (AGAP009246), a chitinase, *Cht24*
461 (AGAP006191), a thioester-containing protein-1, *TEP-1* (AGAP010815),), a trehalose 6-
462 phosphate synthase/phosphatase, *TPS*1/2 (AGAP008227), a lipase (AGAP002353), and
463 AGAP012818 (V-type protein ATPase subunit A). More on these genes is provided in the
464 sections, below.

465 Other genes commonly overexpressed in data from two or three countries include
466 AGAP005501 (dehydrogenase/reductase SDR family 11) upregulated in Nigeria and Niger (R-
467 S and C-S comparisons), and in R-S for Chad and Cameroon; AGAP008091 (CLIP-domain
468 serine protease, *CLIPE1*), upregulated in all countries in R-S and C-S comparisons; a chitinase,
469 *Cht5-5*, AGAP013260) upregulated in Nigeria, Nigeria and Chad R-S and C-S, with both
470 induced upregulated in R-C in Chad, as heme peroxidase (*HPX15*), upregulated in R-S and C-
471 S comparisons in Nigeria, Chad and Cameroon, as well as malate dehydrogenase
472 (AGAP000184), upregulated in Nigeria, Chad and Cameroon, R-S and C-S.

473 However, the most overexpressed genes in Nigeria are a cubilin, a histone (H2B), carbonic
474 anhydrase I, and a cuticular protein, *CPR131* (File S2), while for Cameroon its H2B, Serpin 9
475 inhibitory serine protease inhibitor, galectin 4 and a Protease m1 zinc metalloprotease.

476 Several genes were significantly downregulated across the four countries, particularly the
477 cytochrome P450s and the ATP-binding cassette transporters. The most consistently down-
478 regulated P450s were *CYP6AK1* (AGAP010961), downregulated in R-S and C-S comparisons
479 in Nigeria, Niger and Cameroon, while down-regulated in all comparisons in Chad; *CYP4H24*
480 (AGAP013490), downregulated in R-S and C-S comparisons for Nigeria and Cameroon, and
481 downregulated in all comparisons in Niger and Chad; *CYP6M4* (AGAP008214),
482 downregulated in R-S and C-S comparisons in Nigeria, Niger and Cameroon, while
483 downregulated in all comparisons in Chad; and finally *CYP6P5* (AGAP002866),
484 downregulated in R-S and C-S comparisons in Niger and Chad, but only in C-S in Nigeria.

485

486 *Analysis of commonly overexpressed metabolic resistance genes resistance across the Sahel*

487 Special attention was given to the known metabolic resistance genes, implicated in insecticide
488 resistance in *Anopheles* and/or other insects, including, CYP450s, GSTs, carboxylesterases,

489 cuticular proteins, chemosensory proteins/SAPs, uridine diphosphoglucuronosyltransferases,
490 etc, in addition to other important genes, e.g., the immune proteins. Analysis of the data from
491 the list of genes significantly, differentially expressed (FDR-adjusted $p < 0.05$ and $\log_2 FC = 1/$
492 $FC \geq 2$) revealed the major, commonly upregulated metabolic resistance genes in the four
493 Sahel countries. Top 50 genes from these lists (File S3) from each country are displayed as
494 heatmaps of fold changes in Figure S5a, -b, -c and -d). The most common genes linked with
495 resistance and/or other physiologically important phenotypes are tabulated in Table 1,
496 showing fold changes (R-S and C-S comparisons) of 55 genes, common to all countries, or
497 three or two countries at least. The most commonly and consistently overexpressed genes
498 across the Sahel (taking account mean expressions) are the chymotrypsins, -1, -2 and -3
499 (*CHYM1*/AGAP006709, *CHYM3*/AGAP006711 and *CHYM2*/AGAP006710) (Table 1, Figure S5,
500 File S2 Results), with fold change for *CHYM1* in R-S and C-S comparisons of 31.62 and 54.41
501 for Nigeria, 12.31 and 41.59 for Niger, and 18.00 and 18.08 for Chad, and 5.69 and 11.77 for
502 Cameroon; for *CHYM3*, 32.45 and 58.43 for Nigeria R-S and C-S, respectively, 7.30 and 43.27
503 for Niger, 13.40 and 7.24 for Chad, and 2.59 and 8.15 for Cameroon. Of *Anopheles* metabolic
504 resistance genes, *GSTe2* (AGAP009194) was the most consistently upregulated gene across the
505 Sahel, FC = 9.61 and 7.16, respectively for Nigeria R-S and C-S comparisons; 6.55 and 11.32 for
506 Niger; 9.09 and 10.02 for Chad, 9.68 and 20.67 for Cameroon. Other common GST was *GSTZ1*,
507 upregulated in three countries (Nigeria, Niger and Chad) are *GSTe4*, *GSTU1*, *GSTD1-4* and
508 *GSTD3*.

509 Other most consistently and highly upregulated genes include a lipase (AGAP002353, FC of
510 26.73 and 20.80 for Nigeria R-S and C-S comparisons; 16.53 and 29.76 for Niger, 14.95 and 9.95
511 for Chad, 14.58 and 14.53 for Cameroon); a chitinase, *Cht24* (AGAP006191, FC = 21.12 and
512 38.55 for Nigeria R-S and C-S, 40.08 and 67.18 for Niger, 91.42 and 5.71 for Chad, 44.26 and
513 40.53 for Cameroon); a V-type protein ATPase subunit a (AGAP012818, FC = 22.12 and 14.61
514 for Nigeria, 31.05 and 25.43 for Nigeri, 6.00 and 4.31 for Chad, 44.92 and 43.4 for Cameroon),
515 and an aquaporin, *AQP3* (AGAP010326, FC = 14.81 and 11.03 for Nigeria, 12.09 and 21.94 for
516 Niger, 14.86 and 1.21 for Chad, 14.17 and 17.3 for Cameroon).

517 The most overrepresented gene family, and most consistently upregulated across the Sahel
518 were the cytochrome P450s, with *CYP6Z2*, *CYP6Z3*, and *CYP4C27* taking the front seat, in

519 addition to the two P450s linked to cuticular resistance, *CYP4G16* (upregulated in Nigeria and
520 Chad) and *CYP4G17* (upregulated in Nigeria, Niger and Chad). The three P450s, *CYP6Z2,*
521 *CYP6Z3 and CYP4C27* are consistently overexpressed: FC for *CYP6Z2* is 6.55 and 2.10 for
522 Nigeria R-S and C-S comparisons, 6.73 and 2.32 for Niger, 13.96 and 1.48 for Chad, 11.84 and
523 8.39 for Cameroon; FC for *CYP6Z3* of 4.73 and 1.82 for Nigeria, 6.09 and 1.42 for Niger,
524 3.51 and 1.11 for Chad, 7.11 and 3.79 for Cameroon; and FC for *CYP4C27* is 7.36 and 4.6 for
525 Nigeria, 4.03 and 5.64 for Niger, 6.04 and 2.62 for Chad, 2.01 and 2.63 for Cameroon. The two
526 well-known insecticide resistance genes *CYP6P3* and *CYP9K1* did not future prominently
527 across the Sahel of these countries, neither did *CYP6M2*.

528 The second most commonly overrepresented gene families belong to cuticular proteins,
529 including cuticular proteins Rebers and Riddiford (RR), several cuticular proteins of low
530 complexity (CPLC) and chitin-binding cuticular proteins (CPAP), with the commonly
531 upregulated ones across all four countries being *CPR75* (AGAP009871) and *CPR76*
532 (AGAP009874).

533 Two carboxylesterases picture prominently across the Sahel – the beta esterase, *COEBE3C*
534 (AGAP005372) upregulated in all four countries, while *COEJHE5E* was common to Nigeria,
535 Niger and Chad. For Phase II metabolism enzymes, several uridine-diphospho-
536 glucuronosyltransferases, UGTs were upregulated, including the *UGT-B19*, which is
537 upregulated in Nigeria and Niger (Table 1), and unknown UGT (AGAP006222) upregulated
538 across all the countries (File S2).

539 Other genes in the top 55 metabolic genes include the malate dehydrogenase, *TPS* (*TPS1/2*),
540 *AQP2*, thioester-containing proteins, *TEP1, -12* and *-14*, a cyanogenic-beta-glucosidase
541 (AGAP006422) and three chemosensory proteins, *CSP5*, sensory appendage proteins, -1 and -
542 2.

543

544

545

546

547 **Table 1: Common detoxification and metabolic genes differentially and constitutively**
548 **upregulated in Sahel *An. coluzzii* at FDR-adjusted p < 0.05.**

	NIGERIA		NIGER		CHAD		CAMEROON		
Gene	**R-S**	**C-S**	**R-S**	**C-S**	**R-S**	**C-S**	**R-S**	**C-S**	**Gene Description**
AGAP006400	2.19	4.18	1.72	4.47	-	-	2.11	2.82	alkaline phosphatase 2
AGAP028491	4.34	2.83	1.42	2.66	2.98	2.57	-	-	aquaporin, AQP2
AGAP010326	14.81	11.03	12.09	21.94	14.86	1.21	14.17	17.3	Aquaporin, AQP3
AGAP005372	9.45	12.19	3.34	4.25	6.60	3.62	1.39	2.63	carboxylesterase, COEBE3C
AGAP005837	4.70	5.02	1.41	3.29	1.89	2.64			carboxylesterase, COEJHE5E
AGAP004904	3.88	2.19	-	-	2.34	1.74	-	-	catalase, CAT1
AGAP029127	4.14	3.17	-	-	1.73	2.22	-	-	chemosensory protein 5, CSP5
AGAP006191	21.12	38.55	40.08	67.18	91.42	5.71	44.26	40.53	chitinase, Cht24
AGAP013260	4.40	11.47	1.26	3.89	3.13	0.75	-	-	chitinase, Cht5-5
AGAP006898	8.97	5.52	-	-	2.23	3.93	-	-	chitinase, Cht6
AGAP006709	31.62	54.41	12.31	41.59	18.00	18.08	5.69	11.77	chymotrypsin-1, CHYM1
AGAP006710	9.85	19.44	2.07	8.75	4.21	3.87	-	-	chymotrypsin-2, CHYM2
AGAP006711	32.54	58.43	7.30	43.27	13.40	7.24	2.59	8.15	chymotrypsin-3, CHYM3
AGAP000987	4.28	2.70	-	-	1.34	2.61	-	-	cuticular protein, CPAP3-A1b
AGAP000988	5.33	1.56	-	-	0.74	5.44	-	-	cuticular protein, CPAP3-A1c
AGAP000986	7.31	4.60	-	-	1.73	3.46	-	-	cuticular protein, CPAP3-D
AGAP006149	3.67	0.78	-	-	0.74	5.78	-	-	cuticular protein, CPLCX3
AGAP010123	33.33	54.97	2.35	13.2	-	-	-	-	cuticular protein, CPR131
AGAP010123	33.33	54.97	2.35	13.20					cuticular protein, CPR131
AGAP005456	5.24	1.78	-	-	1.24	2.21	1.07	2.07	cuticular protein, CPR15
AGAP006009	-	-	2.88	1.30	-	-	3.89	1.62	cuticular protein, CPR30
AGAP009871	8.67	2.72	1.07	2.63	2.23	4.18	1.67	2.56	cuticular protein, CPR75
AGAP009874	10.64	2.22	1.05	2.55	3.69	5.56	1.09	2.03	cuticular protein, CPR76
AGAP009879	7.43	2.57	-	-	1.87	4.6	-	-	cuticular protein, CPR81
AGAP006422	7.50	9.41	-	-	8.44	7.33	2.11	1.96	cyanogenic beta-glucosidase
AGAP002417	5.53	4.17	0.95	1.22	1.90	1.87	-	-	cytochrome P450, CYP4AR1
AGAP009246	7.36	4.6	4.03	5.64	6.04	2.62	2.01	2.63	cytochrome P450, CYP4C27
AGAP012957	5.01	2.83	-	-	2.88	2.45	2.04	2.61	cytochrome P450, CYP4D17
AGAP001076	5.79	4.69	1.45	1.80	3.81	2.41	0.88	1.48	cytochrome P450, CYP4G16
AGAP000877	3.81	1.96	2.34	1.85	3.76	2.05	1.20	2.05	cytochrome P450, CYP4G17
AGAP008358	-	-	2.96	4.08	3.43	3.28	3.61	1.99	cytochrome P450, CYP4H17
AGAP007480	5.36	3.99	1.31	2.73	2.49	2.01	-	-	cytochrome P450, CYP6AH1
AGAP002865	1.11	0.50	2.29	1.87	0.66	12.83	2.06	2.26	cytochrome P450, CYP6P3
AGAP008207	3.56	1.96	-	-	2.08	1.64	1.74	2.35	cytochrome P450, CYP6Y2
AGAP008218	6.55	2.10	6.73	2.32	13.96	1.48	11.84	8.39	cytochrome P450, CYP6Z2
AGAP008217	4.73	1.82	6.09	1.42	3.51	1.11	7.11	3.79	cytochrome P450, CYP6Z3
AGAP000818	2.97	1.15	0.75	0.54	0.90	1.59	3.38	2.21	cytochrome P450, CYP9K1
AGAP010400	3.58	2.56	1.62	2.83	3.29	1.44	-	-	flavin-containing monooxygenase
AGAP007920	5.72	2.40	2.84	1.84	-	-	-	-	glucuronosyltransferases, UGT-B19
AGAP004164	2.19	1.85	1.68	2.34	1.39	1.30	-	-	glutathione S-transferase, GSTD1-4
AGAP009194	9.61	7.16	6.55	11.32	9.09	10.02	9.68	20.67	glutathione S-transferase, GSTe2
AGAP009193	3.26	2.29	1.14	2.09	1.46	1.6	-	-	glutathione S-transferase, GSTe4
AGAP000947	4.36	2.31	1.23	2.18	1.91	3.15	-	-	glutathione S-transferase, GSTU1
AGAP002898	5.52	3.51	1.66	2.61	2.76	2.38	-	-	glutathione S-transferase, GSTZ1
AGAP002198	-	-	2.00	5.77	4.75	6.58	-	-	glycine-N-methyltransferase
AGAP013327	-	-	1.16	7.28	7.89	20.11	5.11	14.82	heme peroxidase, HXP15
AGAP002353	26.73	20.80	16.53	29.76	14.95	9.95	14.58	14.53	lipase
AGAP000184	5.16	6.26	-	-	4.87	4.31	1.21	1.90	malate dehydrogenase
AGAP008051	3.65	3.96	1.14	1.30	1.73	1.68	-	-	sensory appendage protein 1, SAP1
AGAP008052	5.47	10.84	1.02	1.45	3.45	1.06	-	-	sensory appendage protein 2, SAP2
AGAP010815	5.68	14.41	4.07	8.55	7.75	3.79	1.65	3.06	thioester-containing protein 1, TEP1
AGAP008368	3.34	6.12	1.39	3.85	3.42	1.97	-	-	thioester-containing protein, TEP14
AGAP008654	4.59	17.36	2.12	10.03	-	-	-	-	thioester-containing protein, TEP12
AGAP008227	4.07	4.00	3.99	2.00	4.59	1.47	2.58	4.12	trehalose 6-phosphate synth/phosph
AGAP012818	22.12	14.61	31.05	25.43	6.00	4.31	44.92	43.4	V-type proton ATPase, subunit a

549 *Gene Ontology Enrichment Analysis*

550 Gene ontology enrichment analysis, for genes significant in comparisons ($log_2FC = 1$, $p < 0.05$)
551 revealed crucial differences in overrepresented GO terms between the up- and -
552 downregulated genes, in data from the four countries. For example, the most over-
553 represented, semantically similar GO terms associated with xenobiotics metabolism is
554 oxidoreductase activity ((highest frequency of 12.9 %, Figure S6a, REVIGO Table View), which
555 cluster together in Nigerian R vs S comparison (for genes upregulated in R). Other over-
556 represented GO terms in this comparison include glutathione S-transferase activity (the most
557 enriched/specific term), peroxidase activity, odorant binding and chitin binding. In contrast,
558 GO terms over-represented in R vs S (down-regulated in R) were mostly involved in
559 neurotransmission, metal ions binding and receptor channelling activities (Figure S6b).

560 For R vs C comparison (upregulated in C) the over-represented GO terms include
561 oxidoreductase (frequency = 12.88 %), glutathione S-transferase activity (the most
562 enriched/specific term), peroxidase activity, glucuronosyltransferase activity, aldehyde
563 oxidase activity, chitin binding, carbohydrate binding activities, etc (Figure S6c). In contrast
564 the most enriched GO terms, downregulated in C were endopeptidase activities, Toll binding,
565 oxidoreductase (frequency = 1.21 %) and monooxygenase activities (Figure S6d). For the rest
566 of the three countries contrasts were also observed, between phenotypes, and detailed in File
567 S1, Results section.

568

569 **Quantitative PCR validation of expression profiles of metabolic resistance genes**

570 The relative expression levels of 12 metabolic resistance genes were validated using the qRT-
571 PCR. The qRT-PCR results support the transcriptomic patterns obtained from the RNAseq
572 analysis, with *GSTe2* as the most overexpressed gene, followed by *CYP6Z2* (Figure 3). For
573 example, for R-S and C-S comparisons *GSTe2* had fold changes of 49.25 ± 5.05 and 28.45 ± 4.45,
574 for Nigeria ($p \leq 0.0001$); 37.01 ± 2.22 and 33.34 ± 6.61 for Niger ($p \leq 0.0001$); 29.97 ± 5.39 and
575 30.16 ± 6.16 for Chad ($p \leq 0.0001$); and 28.30 ± 3.30 ($p \leq 0.0001$) and 17.03 ± 7.03 for Cameroon
576 ($p \leq 0.001$). *CYP6Z2* has R-S and C-S fold changes of 15.93 ± 2.54 ($p \leq 0.001$) and 7.35 ± 1.52
577 ($p \leq 0.05$), for Nigeria; 24.21 ± 2.17 ($p \leq 0.001$) and 20.83 ± 3.02 for Niger ($p \leq 0.001$); 15.02

578 ($p \leq 0.001$) ± 2.01 and 6.09 ± 2.08 for Chad ($p \leq 0.05$); and 10.58 ± 3.00 ($p \leq 0.01$) and 3.43 ± 1.43
579 for Cameroon. Correlation analyses for R-S comparisons for all genes revealed positive and
580 significant association (Figure S7) between the RNA-seq and qRT-PCR data for these genes in
581 data from Niger ($R^2 = 0.58$, p = 0.03) and Chad ($R^2 = 0.408$, p = 0.025), with positive, but non-
582 significance seen in Cameron ($R^2 = 0.58$ p = 0.08) and Nigerian ($R^2 = 0.503$, p = 0.06) data.

583

584 **Detection of Signatures of Selective Sweeps**

585 Signatures of selection were investigated in the major metabolic resistance genes, by
586 estimating Tajima's D per gene within populations, and *F*st per gene between population
587 pairs. These tests of neutrality revealed several genes exhibiting high genetic differentiation,
588 or possibly undergoing expansion. Among the top 100 most overexpressed metabolic genes
589 across the four countries (File S2), 13 genes were possibly undergoing genetic differentiation.
590 These include *TEP1,* and *TEP3*, with average Tajima's D of -1.4 and -1.6 respectively, in
591 populations from Chad, and average *F*st values of 0.58 and 0.49 for all countries (File S3,
592 provide the number of SNPs and chromosomal location for each gene), *CYP9K1* (average
593 Tajima's D = -1.00 for Cameroon, and combined *F*st = 0.55), *CPR15* (average Tajima's D = -
594 0.94, and *F*st = 0.17); *CPAP3-A1b* (Tajima's D = -0.70 in Chad, -0.95 in Nigeria, and -1.32 in
595 Cameroon, with combined *F*st of 0.55) and *CPLCX3*. Several genes from the GST family
596 exhibited strong genetic differentiation with reduced variations prominently in *GSTe2* (< 3
597 SNPs in Chad and Cameroon samples), with Tajima's D of -1.45 and -1.15 for Nigeria and
598 Niger, and combined *F*st of 0.02. Detailed analysis is provided in File S1, and File S3 contain
599 the respective frequencies of these variables.

600

601 **Identificaton of genetics variants associated with insecticide resistance**

602 The RNA-Seq-Pop workflow calculated allele frequencies of variants of interest found in the
603 raw RNA-sequencing read data. Figure 4 displays allele frequencies of each variant in
604 respective treatment replicates used for the RNAseq, as well as Ngoussou. Several mutaions
605 were found within the voltage-gated sodium channel. In addition to the L995F *kdr* mutation,
606 the recently identified V402L and I1527T mutations exist in all the field populations across the

607 Sahel, at frequencies ranging from 29 % to 67 %. We also detected the N1570Y mutation, which
608 shares the same haplotype as L995F. The G280S *acetylcholinesterase*-1 mutation was also
609 observed in low to moderate frequencies in all populations except for Ngoussou and samples
610 from Niger. The L43F pyrethroid resistance marker of *CYP4J5* was also seen, fixed in most
611 populations.

612

613 ***Detection of chromosomal inversion polymorphisms and metabolic genes within the***
614 ***inversion breakpoints***

615 The frequency of the major inversion polymorphisms in chromosome 2 were calculated,
616 considering ploidy (8 individual female mosquitoes were pooled for RNA extraction, for each
617 replicate). Table S5 provided the frequencies of the respective inversions for the populations
618 from each country, as well as for Ngoussou. High frequency of three Anopheles
619 phenotypically important inversions, the 2La, 2Rb and 2Rc, in contrast to the 2Rd, 2Rj and
620 2Ru which were in lower frequencies [except for the 2Rj in Nigeria (30.38 %) and 2Ru in
621 Cameroon (24.29 %)]. The 2La inversion was found fixed in the field populations (100 % in
622 Nigeria and Cameroon, 99.92 % in Niger and 99.21 % in Chad), in contrast with Ngoussou,
623 with frequency of only 6.26 %. Similar pattern was observed with the 2Rb inversion, with high
624 frequencies in three field populations (79.01 %, 84.85 %, 80.22 % in Nigeria, Niger and Chad),
625 but lower in Cameroon (29.08 %) and Ngoussou (5.35 %). Frequencies of the 2Rc inversion
626 were 88.54 %, 85.52 %, 88.82 %, 46.99 % and 9.89 % for Nigeria, Niger, Chad, Cameroon and
627 Ngoussou respectively. Some genes among the top 100 most overexpressed metabolic
628 resistance genes (above) and which were likely undergoing recent population expansion were
629 located within the 2La, 2Rb and 2Rc inversions (File S4). These include the *hsp83*
630 (AGAP006958) and molecular chaperone hptG (AGAP006961), *CPLCX3* (AGAP006149),
631 *CPLCA1* (AGAP006145,) within the inverted 2La chromosomal arm. Other genes within 2La
632 inversion include a group of chitinase enzymes (*Cht6*, *-8*, *-11* and *-24*, most notably the *Cht24*
633 and *Cht6*, which are among the top 50 most overexpressed genes in all countries. Other genes
634 include *COEJHE5E*, one of the 14 carboxylesterases in the 2La region, and which was among
635 the top 100 most overexpressed genes across the Sahel; the most overexpressed chymotrypsin
636 genes, *CHYM1* and *CHYM2*; three ionotropic receptors, *IR136* (AGAP006440), *IR139*

637 (AGAP006691) and *IR142* (AGAP006407); as well as five P450s, *CYP301A1*, *CYP302A1*,
638 *CYP4J5*, CYP4J9 and *CYP4J10*. The most overrepresented genes within 2La inversions are the
639 CPR cuticular proteins (73 in total), with *CPR21*, *-26*, *-30*, *-59* and *-140* from the list of the top
640 100 resistance genes from the Sahel.
641 Carbonic anhydrase I (the most overexpressed metabolic resistance in Nigeria, AGAP013402
642 is sit within 2Rb inversion region). Four chitinases (*Cht4*, *Cht5-1*, *Cht5-3*, and *Cht5-5*) are
643 located within 2Rb inversion; *Cht5-1* and *Cht5-5* were among the observed top 50 most
644 overexpressed metabolic genes in the Sahel. Lipase (*AGAP002353*) which is the among the top
645 6 overexpressed metabolic gene in the four countries sit within the 2Rb inversion. Eight
646 CYP450s reside in the 2Rb inversion, including *CYP4D15*, *CYP4D17* and *CYP4AR1*, which
647 were among the top 100 metabolic resistance genes. Three cuticular proteins, *CPR7*, *-8* and *-9*
648 were also within the 2Rb inversion.

649 Interesting genes sitting within 2Rc inversion include *GSTZ1*; 5 ionotropic receptor genes, *IR7i*
650 (AGAP013363), *IR7u* (AGAP013285), *IR7t* (AGAP002763), *IR7w* (AGAP013416) and *IR41a*
651 (AGAP002904); a carboxylesterase, *COEAE6O* (AGAP002863); and 11 CYP450s, including
652 *CYP6AA1* (AGAP002862), *CYP6AA2* (AGAP013128), *CYP6P15P* (AGAP002864), *CYP6P3*
653 (AGAP002865), *CYP6P5* (AGAP002866), *CYP6P4* (AGAP002867), *CYP6P1* (AGAP002868),
654 *CYP6P2* (AGAP002869), *CYP6AD1* (AGAP002870) and *CYP6Z4* (AGAP002894)

655

656 ***Investigation of the polymorphism in the coding sequences of Sahelian GSTe2 and CYP6Z2***

657 Analysis of the polymorphism patterns of full-length cDNA sequences of *GSTe2* (666 bp) and
658 *CYP6Z2* (1479 bp) from the Sahel region of Africa revealed complete homogeneity for *GSTe2*,
659 with no single polymorphism detected in the field populations as well as Ngoussou (all
660 sequences identical to AGAP009194 reference). This suggests a fixed allele, consistent with the
661 observation from the analyses from the fixation index (File S3). For *CYP6Z2* (1479 bp),
662 homogeneity was observed within each country and Ngoussou, except for Niger,
663 characterised by an unusually high polymorphism (Figure S8a, -b). *CYP6Z2* is polymorphic
664 with 10 haplotypes across the Sahel, with 75 polymorphic sites of which 65 were synonymous,
665 and 12 led to amino acids substitutions. The bulk of the polymorphisms were contributed
666 from larger variations in the Niger and Cameroon (S = 42 and 23 respectively), while highest

667 homogeneity was observed in Chad, with a single haplotype. Haplotype diversity is high
668 (H_d = 0.921), from 10 haplotypes out of only 20 sequences, with the lowest H_d in the Chad
669 sequences, suggesting a directional selection/fixed allele. The haplotypes cluster according to
670 origin on the maximum likelihood phylogenetic tree, except for Niger (Figure S8c).

671

672 ***Investigation of the role of intergenic region regulatory elements in overexpression of GSTe2***
673 ***and CYP6Z2***

674 *Investigation of polymorphism in the intergenic region/regulatory elements*

675 To investigate polymorphisms in the regulatory elements of the above genes, the 351
676 intergenic regions of *GSTe2* (spanning the 43 bp 3′-UTR of *GSTe1,* 248 bp flanking sequence
677 and 60 bp 5′-UTR of *GSTe2*) preceding the start codon were amplified from 10 each of DDT-
678 alive and -dead females from the 4 Sahel countries, as well as from Ngoussou females,
679 successfully. For *CYP6Z2,* 1078 bp (spanning 38 bp 3′ UTR of *CYP6Z1,* 937 bp flanking
680 sequence and 103 bp 5′UTR of *CYP6Z2,* preceding the start codon of *CYP6Z2*) were used to
681 amplify fragments from 10 each of deltamethrin-alive and -dead females from Nigeria, and
682 from Ngoussou females.

683 Out of the 90 *GSTe2* 5′-UTR sequences analysed differences were observed between the alive
684 and dead mosquitoes, with a total of 65 sequences from alive and dead females (regardless of
685 country of origin) identical to the 10 sequences of Ngoussou. From the 40 sequences of the
686 dead females, 39 were identical to Ngoussou (regardless of the country). Twelve sequences,
687 all from the alive females (from across the four countries) were similar, with several mutations
688 in putative transcriptional factors binding sites, which may impact overexpression of the
689 *GSTe2.* In short, 8 mutations were shared in common between these 12 sequences of DDT-
690 alive females from across the countries (3 each from Nigeria, Chad and Cameroon) and
691 additional mutations in the Niger samples (4 sequences). These mutations include (i) T->A
692 transition withing the cellular myb-DNA (c-myb) binding domain (Figure S9), (ii) a T->C
693 transversion in the zinc-finger homeodomain, δEF1 (δ elongation factor 1) binding site, (iii) T-
694 >A transition in the nuclear matric protein 4 (NMP4), (iv) simultaneous insertion of adenine
695 and a transition T -> C, in positions 113 and 114 respectively, between the Fork-head box L1

696 and c-EST binding sites, (v) an A -> C transversion in a second NMP4, (vi) a T -> C transition,
697 six nucleotides downstream the nuclear factor κB (NF-κB), (vii) followed by an A -> G
698 transversion 3 nucleotides downstream the NF-κB, (viii) a G -> A transversion, 7 nucleotides
699 upstream the GC box, (ix) a C -> G transition, 2 nucleotides downstream the arthropod
700 initiator (Inr consensus) sequence, and finally (x) a C -> G transition, within the 5′-UTR of the
701 *GSTe2*, 28 nucleotides downstream the transcriptional start site/49 nucleotides upstream the
702 *GSTe2*, start codon.

703 Analysis of the 90 sequences revealed a very low polymorphism in the dead mosquitoes (S =
704 0, for Niger-dead, Chad-dead and Ngoussou), but high polymorphism in the alive (S = 16 for
705 Nigeria-alive, and 13 each for Chad-alive and Cameroon-alive) (Table S6). All sequences
706 produced 17 polymorphic sites, with 6 haplotypes (Figure S10a and -b). High haplotype
707 diversities were obtained from the alive mosquitoes (for example, Nigeria alive, Hd = 0.71,
708 Niger-alive 0.53). Regardless of country of origin, the haplotypes cluster according to
709 phenotype on the maximum likelihood phylogenetic tree, with the alive haplotypes forming
710 a distinct/separate clade (Figure S10c).

711 With regard to *CYP6Z2* no major differences were observed when comparing the
712 deltamethrin-alive and -dead sequences with the Ngoussou.

713

714 *Comparative measurement of activities of the 5′ regulatory elements of the GSTe2 and CYP6Z2*

715 Initial promoter analyses were conducted with the 5′- regulatory element sequences of *GSTe2*,
716 for the DDT-alive females (representative sequence with the 8 common polymorphic
717 positions, designated, Sahel-alive), comparing it with the sequence from the DDT-
718 dead/Ngoussou (designated Ngoussou/Sahel-dead). For *CYP6Z2*, a predominant sequence
719 from the Nigeria field sample (with 8 nucleotide insertion) was compared with the Ngoussou
720 sequence.

721 The ability to drive heterologous expression of the firefly luciferase was determined, with the
722 Sahel-alive construct and Ngoussou/Sahel-dead producing increased luciferase activity
723 [~3090× (normalized luciferase activity = 2.58) and 479× (normalized activity = 0.400),
724 respectively] compared with the promoter pGL3-Basic vector. But the Sahel-alive construct

725 was significantly more active than the Ngoussou/Sahel dead counterpart [promoter activity
726 ~6-fold higher (Tukey HSD Q = 8.11, p = 0.004)]. In contrast, for *CYP6Z2* no significant
727 differences were observed when comparing the field construct (normalized luciferase activity
728 = 5.95 for alive/dead field construct), compared with 5.84 for the Ngoussou construct.

729

730 *GSTe2 promoter delineation and measurement of activity*

731 Sequential deletion of the intergenic region of the *GSTe2* resulted in progressive reduction in
732 luciferase activity. Deletion of the 43 bp 3′-UTR of the *GSTe1* (-308 from the start codon of
733 *GSTe2*) reduced activity of the Sahel-alive construct by only 18.6 % suggesting that the c-Myb
734 transcriptional factor binding site may not be critical for overexpression (Figure 5). Deletion
735 of an additional 38 nucleotides from the flanking region (-270 fragment, obliterating the δEF1
736 binding site) had comparable impact as above, with activities reducing by 15.3 % only.
737 Removing the *GSTe-1* 3′-UTR and an additional 46 nucleotides from the flanking region (-262
738 fragment, which obliterated in addition the FOX-L1 putative binding site) reduced activity by
739 64.1 % (Q = 6.18, p = 0.01) indicating the importance of this binding site. Deletion of *GSTe1* 3′-
740 UTR plus 75 nucleotides of the flanking region (-232 fragment, located 10 nucleotides from
741 the c-EST binding site) significantly reduced the activity by ~70% (Q = 6.14, p = 0.01),
742 suggesting the importance of the simultaneous insertion of adenine and transition of T to C,
743 in position 113 and 114 respectively, between the FOX-L1 and c-EST binding sites. Removing
744 the fragment of the 5′UTR of *GSTe2* (43 nucleotides preceding the AUG codon obliterated the
745 promoter activity, reducing the luciferase expression by 98 % (Q = 9.41, p = 0.002). This is
746 despite presence of all the above binding sites and transcriptional start site in this fragment.
747 Deletion of the 5′-UTR from Ngoussou significantly reduced activities as well (reduction by
748 88 % compared with the full Ngoussou intergenic region construct, Q = 13.75, p = 0.001).
749 Overall, these findings suggest that the essential binding sites for overexpression of *GSTe2*
750 span the FOX-L1 and c-EST binding sites, with the 5′-UTR essential for activity.

751

752

753 ***Investigating the role of GSTe2 and CYP6Z2 in insecticides resistance using transgenic***
754 ***analysis***

755 A qRT-PCR was conducted using the transgenic flies to first establish overexpression of the
756 above genes. Relative fold changes (FC) of 32.7 ± 4.6 and 25.30 ± 2.8 were obtained in flies
757 overexpressing the *GSTe2* and *CYP6Z2* respectively, compared with control flies (progenies
758 of crosses between the parental line flies with no gene insertion, crossed with GAL4/UAS
759 driver line) (Figure S11).

760 Contact bioassays carried out using 0.05 % α-cypermethrin revealed a high susceptibility in
761 the transgenic flies expressing *GSTe2* (Act5C-GAL4-UAS-GSTe2) and controls (Figure 6a),
762 with mortalities increasing from 62 % and 70 % respectively in 1 h, to 94 % and 99 % in 24 h.
763 However, significantly reduced mortalities were observed in transgenic flies expressing
764 *CYP6Z2* (Act5C-GAL4-UAS-CYP6Z2) compared to control flies, at 1 h (mortality = 35 % *vs* 70
765 % in control, $p < 0.001$) and 3 h (mortality = 52 % vs 89 % in the control, $p < 0.001$). High
766 susceptibilities were also seen in all the experimental flies exposed to 0.05 % deltamethrin,
767 except for 1 h with flies expressing *CYP6Z2* (mortality = 47 % compared with 58 % in the
768 control flies, $p < 0.010$). The *GSTe2* transgenic flies were highly resistant to 2 % permethrin,
769 with no mortality at all in 1 h (Figure 6b), and average mortalities of only 8.5 % at 24 h ($p <$
770 0.0001), compared with 85 % at 1 h for control flies, which increased to 100 % from 3 h.

771 Initial exposure to 4 % of 3-phenoxybenzaldehyde (PBAld) and 3-phenoxybenzyl alcohol
772 (PBAlc) had no toxic effect on flies (Figure not shown). However, 5x concentration of these
773 primary products of pyrethroid hydrolysis induced mortalities, albeit low in all flies (Figure
774 6c). For PBAld, mortalities ranged from 15.5 % and 17.5 % at 1 h, for *CYP6Z2* transgenic flies
775 and control flies respectively, to 30 % and 27.5 % at 24 h. Although low mortalities were
776 observed as well with PBAlc, but at 1 h and 3 h exposure times the mortalities in the transgenic
777 flies expressing *CYP6Z2* were significantly lower compared with mortalities from the control
778 flies (1 h mortality = 2.5 % *vs* 12.5 %, $p < 0.001$; 3 h mortality = 9.5 % *vs* 17.5 %, $p < 0.001$).

779 Marginal tolerance towards DDT was observed in the *CYP6Z2* transgenic flies when
780 compared with the control flies, but only at 3 h ($p < 0.001$) and 6 h ($p < 0.01$) (Figure 6d). This
781 is in contrast with the *GSTe2* transgenic flies, with very low mortalities, in ranges of 0 % to

782 9.52 % for 1 h to 24 h, when compared with control flies (mortality = 34 % in 1 h and 100 % in
783 6 – 24 h, $p < 0.0001$).

784 Susceptibility to clothianidin was very high (Figure 6d), but surprisingly the *CYP6Z2*
785 transgenic flies exhibited a contrasting phenotype, with significantly higher mortalities
786 compared with the control flies, at 1 h (mortality = 67 % vs 42 %, $p < 0.001$), 3 h (mortality = 71
787 % vs 53 %, $p < 0.001$) and 6 h (mortality = 78 % vs 62 %, $p < 0.01$).

788 Taken together, these results confirmed that over-expression of *GSTe2* alone is sufficient to
789 confer resistance to type I pyrethroid (permethrin) and DDT, while overexpression of *CYP6Z2*
790 alone, may confer marginal resistance to the α-cypermethrin and PBAlc.

791

792 **Discussion**

793 Escalating insecticide resistance across Africa (Ibrahim et al., 2019b, Riveron et al., 2019, Toe
794 et al., 2015, Riveron, 2018), if not tackled, will probably compromise the malaria control and
795 elimination efforts. Molecular markers of metabolic resistance e.g., (Lucas et al., 2019,
796 Mugenzi et al., 2019, Weedall et al., 2019), will support evidence-based control and resistance
797 management. Identification and validation of resistance markers in malaria vectors across
798 regions of sub-Saharan Africa can promote communication, cooperation and coordination
799 among malaria control/elimination programs, and allow control efforts to be tailored to the
800 vector species involved in transmission across borders (Shiff, 2002), and tracking of the
801 evolution and spread of resistance markers across regions (Riveron et al., 2014b). To support
802 malaria pre-elimination efforts in Africa, in this study we targeted the Sudan savannah and
803 Sahel (regions of Africa sharing similar eco-climatic conditions, and characterised by high
804 seasonal transmission), which are ideal for control and elimination of malaria using seasonal
805 vector control (Cairns et al., 2012) and chemoprevention.

806

807 ***Anopheles coluzzii* is a major malaria vector across the Sudano-Sahelian transects**

808 Contrary to the previous observations that *An. arabiensis* tends to predominate in arid
809 savannas, while *An. gambiae* is the dominant species in humid forest zones (Lindsay, 1998,

810 Coetzee, 2000, Ranson et al., 2009), *An. coluzzii* has repeatedly been identified as the major
811 malaria vector in the Sudan savannah and Sahel of several, neighbouring countries (including
812 in northern Nigeria, southern Niger, central Chad, and northern Cameroon) (Ibrahim et al.,
813 2019a, Ibrahim et al., 2019b, Ibrahim et al., 2019c, Fadel et al., 2019, Ibrahim et al., 2021) in
814 recent years, suggesting that this vector has adapted well in drier regions of the Sahel
815 transects, and is probably predominating over *An. arabiensis* and *An. gambiae s.s*. This is not
816 surprising as this species exhibits higher exploitation of breeding sites associated with
817 anthropogenic activities, and behavioural plasticity to avoid predators (Gimonneau et al.,
818 2010), and is known to survive a long dry season *in situ*/aestivation, which allows it to
819 predominate, becoming the primary force of malaria transmission (Dao et al., 2014, Lehmann
820 et al., 2017). Also, photoperiod and lower nightly temperature have been shown to
821 significantly increase the longevity of the *An. coluzzii*; mechanisms which allow it to diapause
822 in the dry season and re-establish first in the early rainy season (Huestis et al., 2017).

823

824 **Common metabolic genes mediate multiple resistance in the Sahelian *An. coluzzii***

825 Several genes shown to confer metabolic resistance in *Anopheles* mosquitoes and other insects
826 were found constitutively overexpressed and/or induced in this study. *GSTe2* (AGAP009194)
827 is one of the most regularly encountered metabolic genes in resistant populations of the major
828 malaria vectors *An. gambiae*, *An. coluzzii* and *An. funestus* (Lucas et al., 2019, Mitchell et al.,
829 2014, Riveron et al., 2014b, Menze et al., 2020). This gene has been validated in conferring
830 resistance to DDT (Mitchell et al., 2014) and fenitrothion (Adolfi et al., 2019) in *An. gambiae*. It
831 was extensively studied in *An. funestus*, in which it was shown to confer cross-resistance to
832 DDT and permethrin (Riveron et al., 2014b), reduce efficacy of the LLINs, PermaNet 2.0 and
833 PermaNet 3.0 (side panels) (Menze et al., 2020), and even increase the longevity of the resistant
834 populations carrying the 119F mutation (Tchouakui et al., 2018). These and our findings
835 suggest that the overexpression of this GST alone confer resistance to three insecticides from
836 three different classes (DDT, permethrin and fenitrothion).

837 Several cytochrome P450s previously linked with insecticide resistance were found
838 overexpressed across the Sahel. For example, *An. gambiae CYP6Z2* (AGAP008218) known to
839 metabolize carbaryl (Chiu et al., 2008), the insect juvenile hormone analogue insecticide,

840 pyriproxyfen (Yunta et al., 2016) and mitochondrial complex I inhibitors, fenazaquin,
841 pyridaben and tolfenpyrad (Lees et al., 2020). This P450 also plays a pivotal role in the
842 clearance of pyrethroid insecticides via further catabolism of pyrethroid derivatives (PBAld
843 and PBAlc) obtained by the action of carboxylesterases (Chandor-Proust et al., 2013), in line
844 with our findings of this gene conferring marginal resistance to PBAlc and α-cypermethrin.
845 However, our findings suggest that overexpression of this P450 may enhance the efficacy of
846 clothianidin, which will be epidemiologically advantageous in terms of control. Indeed,
847 bioactivation by P450s is known to be a requirement for insecticidal toxicity of several classes
848 of insecticides, e.g., the organophosphates and chlorpenafyr. Other important CYP450s found
849 to be commonly overexpressed across the Sahel include the *CYP4C27* (AGAP009246), *CYP6Z3*
850 (AGAP008217) and *CYP9K1* (AGAP000818), all three shown to be consistently overexpressed
851 in field populations of *An. gambiae/coluzzii* and *An. funestus* across Africa (Antonio-Nkondjio
852 et al., 2016, Toe et al., 2015, Riveron et al., 2017). *CYP9K1* has been shown to be
853 epidemiologically important pyrethroid-metabolising P450 linked with metabolism of
854 deltamethrin and pyriproxyfen (Vontas et al., 2018).

855 Several carboxylesterases were also upregulated/induced across the Sahel, with the *COEBE3C*
856 (AGAP005372) upregulated in all four countries. This beta esterase is enriched in the legs
857 (where xenobiotic detoxification probably occur) of pyrethroid-resistant *An. coluzzii* (Kefi et
858 al., 2021). Other genes consistently overexpressed across the Sahel, include the chymotrypsin
859 genes (*CHYM3*/AGAP006711 and *CHYM1*/AGAP006709) and a lipase (AGAP002353).
860 Chymotrypsins are known to defend insects against plants' proteinase inhibitors (Dunse,
861 2010); and previous transcriptional studies have shown *CHYM1* and *CHYM3* overexpressed
862 in insecticide resistant populations of *An. gambiae* and *An. coluzzii,* respectively (Toe et al.,
863 2015, Antonio-Nkondjio et al., 2016). Using *in vitro* and *in vivo* tools, lipases have been linked
864 with deltamethrin resistance in *Culex pipiens* pallens (Hu et al., 2020).

865

866 **Common metabolic resistance markers probably exacerbate resistance across the Sahel**

867 Several well-known genetic variants implicated in resistance, as well as the recently
868 discovered ones exist in high frequencies in the Sahelian *An. coluzzii*. For example, the
869 pyrethroid resistance L43F marker of *CYP4J5* (Weetman et al., 2018) was found fixed across

870 the Sahel. The G280S/G119S *ace*-1 mutation, found in high frequencies across Sahel confers
871 organophosphate an carbamates resistance (Weill et al., 2004), and is shown recently to confer
872 resistance to pirimiphos-methyl, in *An. coluzzii/gambiae* (Grau-Bove et al., 2021). Several
873 mutations found within the VGSC have recently been described/validated. For example, the
874 resistance mutation, L995F (Williams et al., 2022) and the V402L/I15227T haplotypes have
875 been observed across Africa (Clarkson et al., 2021). Recently, the two mutations
876 (V402L/I15227T) are described to be in tight linkage and mutually exclusive to the classical
877 L995F/S mutations (Williams et al., 2022), but our results suggest haplotypes carrying the
878 V402L/I1527T combination plus the L995 replacement do exist in the Sahel *An. coluzzii*. Not
879 only that, it is also in addition to the N1570Y replacement.

880

881 **Evidence of cuticular resistance mechanism in the Sahelian *An. coluzzii***

882 Our results suggest cuticular mechanism playing role in pyrethroid resistance in these
883 populations. For example, the findings of *CYP4G16* (AGAP001076) and *CYP4G17*
884 (AGAP000877) overexpressed across the Sahel. The former P450 was previously shown to be
885 involved in epicuticular hydrocarbon biosynthesis associated with resistance (Balabanidou et
886 al., 2016).

887 The three major classes of the insect cuticular proteins - the CPR, CPLC and CPAP, were found
888 overrepresented in the top overexpressed genes across the Sahel, with the commonly
889 upregulated ones being *CPR76*, *CPR15* and *CPR30*, and with the *CPR15*, a chitin-binding
890 cuticular protein, *CPAP3-A1b*, and cuticular proteins of low complexity, *CPLCX3* and
891 *CPLCA1*. Indeed, *CPAP3-A1b* (AGAP000987) have been shown to be highly overexpressed in
892 deltamethrin-resistant Sahelian population of *An. coluzzii* from Burkina Faso (Toe et al., 2015)
893 and induced by blood feeding in *An. gambiae* (Vannini et al., 2014). The CPR and CPLC
894 cuticular proteins have been described to potentially play a crucial role in insecticide
895 resistance through leg cuticle remodelling/thickening, regulating penetration rate of
896 insecticides in *An. coluzzii* (Kefi et al., 2021). Furthermore, a recent study has found most of
897 the cuticular proteins we have described here, as highly overexpressed in
898 permethrin/malathion resistant populations of Ethiopian *An. arabiensis* (Messenger et al.,
899 2021), e.g., *CPR30*, *CPR75*, *CPR81*, and *CPLCP11*. Out of the several chitinases overexpressed

900 across the Sahel, four were amongst the top 50 most overexpressed metabolic genes. These
901 include the *Cht24* (AGAP006191) and *Cht6* (AGAP006898) that have been shown to be
902 overexpressed in the *An. arabiensis* from the above study (Messenger et al., 2021), with the
903 ortholog of *Cht24*, AARA007329 among the top 10 most overexpressed genes in *An. arabiensis*,
904 in line with our observations in *An. coluzzii* across the Sahel. There is an overwhelming need
905 to functionally investigate the role/contribution towards insecticide resistance of these
906 cuticular proteins, chitinases and a chitin synthase (AGAP001748) significantly overexpressed
907 in the field *An. coluzzii* from Nigeria and Chad.

908

909 **Evidence of insecticide resistance- and thermotolerance-associated genes sitting within**
910 **chromosomal inversions**

911 In this study, the findings of high frequency of 2La, 2Rb and 2Rc inversion polymorphisms in
912 the resistant field populations of *An. coluzzii* across the Sahel, compared with the Ngoussou,
913 suggested strong phenotypic adaptations in this species, across the Sahel. Most importantly,
914 in addition to several of the cuticular protein genes associated with resistance (chitinases,
915 chitin synthase, CPR, CPLC and CPAP proteins), several other genes previously implicated
916 in thermotolerance and/or desiccation resistance in *An. gambiae/coluzzii,* and which were
917 highly overexpressed in this study sit within these inversions. For example, the heat shock
918 proteins, *hsp83* (AGAP006958) and *hsp90* hptG (AGAP006961), both of which are known to be
919 heat and insecticides stress inducible (Zhao, 2012) and were among the core set of hsp genes
920 involved in a common and immediate response to thermal stress in *An. gambiae* populations
921 (Cassone et al., 2011) sit within the 2La inversion. These two genes were among the
922 overexpressed genes in both heat-hardened and permethrin-resistant *An. coluzzii* populations
923 from northern Nigeria (Ibrahim et al., 2021). Several ionotropic glutamate receptors were
924 found within the 2La inversion breakpoints: *IR136* (AGAP006440), *IR139* (AGAP006691) and
925 *IR142* (AGAP006407). This is not surprising as ionotropic receptors are commonly associated
926 with chemosensation, thermosensation, and hygrosensation (VanHook, 2016, Enjin et al.,
927 2016), characteristics which can confer advantages in xeric environments.
928 The *IR25a* (AGAP010272) and *IR21a* (AGAP008511) are known to mediate both humidity and
929 temperature preference in the fruit fly, *D. melanogaster* (Enjin et al., 2016, Greppi et al., 2020),

930 in addition to *IR21a* driving heat seeking and heat-stimulated blood feeding in *An.*
931 *gambiae* (Greppi et al., 2020), with both shown to be overexpressed/induced in
932 thermotolerant/permethrin resistant populations of *An. coluzzii* (Ibrahim et al., 2021).

933

934 **Conclusions**

935 Information on molecular basis of resistance and/or resistance genes and its markers facilitates
936 evidence-based control measures. In this study we characterised a major malaria vector, *An.*
937 *coluzzii* from the Sahel region of four countries, with findings which could promote evidence-
938 based, cross-border policy towards local and regional malaria control. The study found that
939 across Sahel (where malaria is highly seasonal, reaching its peak in the rainy season), the major
940 malaria vector is *An. coluzzii*. And that a handful of common cross-resistance genes are
941 responsible for multiple insecticide resistance in this species. Findings from this study suggest
942 pleotropic role of some key genes – able to confer insecticide resistance and/or stabilize the
943 insecticide resistance gene, at the same time conferring environmental adaptations, such as
944 the ability to survive thermal stress (thermotolerance). From operational vector control
945 perspective this study provided evidence of the role of key insecticide metabolism gene,
946 *CYP6Z2* in bioactivation of a major insecticide, clothianidin, into more insecticidal
947 intermediates, which could increase the efficacy of the ingredients in malaria control tools
948 utilizing it to target field populations overexpressing this key P450.

949

950 **Data Availablity**

951 The raw sequence reads from this study have been deposited in the European Nucleotide
952 Archive, with accession PRJEB51644, and secondary accession of ERP136291.

953

954 **Conflict of Interest**

955 The authors declare no conflict of interest.

956

957 **Acknowledgments**

958 A Wellcome Trust International Training Fellowship in Public Health and Tropical Medicine
959 (WT201918/Z/16/Z) to SSI supported this work.

960

961

962 **Reference**

963 ADOLFI, A., POULTON, B., ANTHOUSI, A., MACILWEE, S., RANSON, H. & LYCETT, G. J. 2019. Functional
964 genetic validation of key genes conferring insecticide resistance in the major African malaria
965 vector, Anopheles gambiae. *Proc Natl Acad Sci U S A,* 116**,** 25764-25772.
966 ALEXA A., R. J. 2021. *topGO: Enrichment Analysis for Gene Ontology. R package version 2.46.0.*
967 [Online]. [Accessed].
968 ALISTAIR MILES, M. F. R., PETER RALPH, NICK HARDING, RAHUL PISUPATI, AND SUMMER RAE. 2020.
969 *cggh/scikit-allel: A Python package for exploring and analysing genetic variation data*
970 [Online]. [Accessed].
971 ANOPHELES GAMBIAE GENOMES, C., DATA ANALYSIS, G., PARTNER WORKING, G., SAMPLE, C.-A.,
972 BURKINA, F., CAMEROON, GABON, GUINEA, GUINEA, B., KENYA, UGANDA, CROSSES,
973 SEQUENCING, DATA, P., WEB APPLICATION, D. & PROJECT, C. 2017. Genetic diversity of the
974 African malaria vector Anopheles gambiae. *Nature,* 552**,** 96-100.
975 ANTONIO-NKONDJIO, C., POUPARDIN, R., TENE, B. F., KOPYA, E., COSTANTINI, C., AWONO-AMBENE,
976 P. & WONDJI, C. S. 2016. Investigation of mechanisms of bendiocarb resistance in Anopheles
977 gambiae populations from the city of Yaounde, Cameroon. *Malar J,* 15**,** 424.
978 ARONESTY, E. 2011. ea-utils: Command-line tools for processing biological sequencing data. Durham,
979 NC.
980 BALABANIDOU, V., KAMPOURAKI, A., MACLEAN, M., BLOMQUIST, G. J., TITTIGER, C., JUAREZ, M. P.,
981 MIJAILOVSKY, S. J., CHALEPAKIS, G., ANTHOUSI, A., LYND, A., ANTOINE, S., HEMINGWAY, J.,
982 RANSON, H., LYCETT, G. J. & VONTAS, J. 2016. Cytochrome P450 associated with insecticide
983 resistance catalyzes cuticular hydrocarbon production in Anopheles gambiae. *Proc Natl Acad*
984 *Sci U S A,* 113**,** 9268-73.
985 BARNES, K. G., WEEDALL, G. D., NDULA, M., IRVING, H., MZIHALOWA, T., HEMINGWAY, J. & WONDJI,
986 C. S. 2017. Genomic Footprints of Selective Sweeps from Metabolic Resistance to
987 Pyrethroids in African Malaria Vectors Are Driven by Scale up of Insecticide-Based Vector
988 Control. *PLoS Genet,* 13**,** e1006539.
989 BHATT, S., WEISS, D., CAMERON, E., BISANZIO, D., MAPPIN, B., DALRYMPLE, U., BATTLE, K., MOYES,
990 C., HENRY, A. & ECKHOFF, P. 2015. The effect of malaria control on Plasmodium falciparum
991 in Africa between 2000 and 2015. *Nature,* 526**,** 207.
992 BLIGHE, K., S. RANA, AND M. LEWIS. 2018. "EnhancedVolcano: Publication-ready volcano plots with
993 enhanced colouring and labeling.".
994 BRUCE-CHWATT, L. J. 1951. Malaria in Nigeria. *Bulletin of the World Health Organization,* 4**,** 301-327.
995 CAIRNS, M., ROCA-FELTRER, A., GARSKE, T., WILSON, A. L., DIALLO, D., MILLIGAN, P. J., GHANI, A. C.
996 & GREENWOOD, B. M. 2012. Estimating the potential public health impact of seasonal
997 malaria chemoprevention in African children. *Nat Commun,* 3**,** 881.
998 CARTHARIUS, K., FRECH, K., GROTE, K., KLOCKE, B., HALTMEIER, M., KLINGENHOFF, A., FRISCH, M.,
999 BAYERLEIN, M. & WERNER, T. 2005. MatInspector and beyond: promoter analysis based on
1000 transcription factor binding sites. *Bioinformatics,* 21**,** 2933-42.

1001 CASSONE, B. J., MOLLOY, M. J., CHENG, C., TAN, J. C., HAHN, M. W. & BESANSKY, N. J. 2011.
1002 Divergent transcriptional response to thermal stress by Anopheles gambiae larvae carrying
1003 alternative arrangements of inversion 2La. *Mol Ecol,* 20**,** 2567-80.
1004 CHANDOR-PROUST, A., BIBBY, J., REGENT-KLOECKNER, M., ROUX, J., GUITTARD-CRILAT, E.,
1005 POUPARDIN, R., RIAZ, M. A., PAINE, M., DAUPHIN-VILLEMANT, C., REYNAUD, S. & DAVID, J.
1006 P. 2013. The central role of mosquito cytochrome P450 CYP6Zs in insecticide detoxification
1007 revealed by functional expression and structural modelling. *Biochem J,* 455**,** 75-85.
1008 CHIU, T. L., WEN, Z., RUPASINGHE, S. G. & SCHULER, M. A. 2008. Comparative molecular modeling of
1009 Anopheles gambiae CYP6Z1, a mosquito P450 capable of metabolizing DDT. *Proc Natl Acad*
1010 *Sci U S A,* 105**,** 8855-60.
1011 CLARKSON, C. S., MILES, A., HARDING, N. J., O'REILLY, A. O., WEETMAN, D., KWIATKOWSKI, D.,
1012 DONNELLY, M. J. & ANOPHELES GAMBIAE GENOMES, C. 2021. The genetic architecture of
1013 target-site resistance to pyrethroid insecticides in the African malaria vectors Anopheles
1014 gambiae and Anopheles coluzzii. *Mol Ecol,* 30**,** 5303-5317.
1015 COETZEE, M., CRAIG, M. AND LE SUEUR, D. 2000. Distribution of African malaria mosquitoes
1016 belonging to the Anopheles gambiae complex. *Parasitology today,* 16**,** 74-77.
1017 COLUZZI, M., SABATINI, A., PETRARCA, V. & DI DECO, M. A. 1979. Chromosomal differentiation and
1018 adaptation to human environments in the Anopheles gambiae complex. *Trans R Soc Trop*
1019 *Med Hyg,* 73**,** 483-97.
1020 DAO, A., YARO, A. S., DIALLO, M., TIMBINE, S., HUESTIS, D. L., KASSOGUE, Y., TRAORE, A. I., SANOGO,
1021 Z. L., SAMAKE, D. & LEHMANN, T. 2014. Signatures of aestivation and migration in Sahelian
1022 malaria mosquito populations. *Nature,* 516**,** 387-90.
1023 DUNSE, K. M., KAAS, Q., GUARINO, R.F., BARTON, P.A., CRAIK, D.J. AND ANDERSON, M.A. 2010.
1024 Molecular basis for the resistance of an insect chymotrypsin to a potato type II proteinase
1025 inhibitor. *Proceedings of the National Academy of Sciences,* 107**,** 15016-15021.
1026 ENJIN, A., ZAHARIEVA, E. E., FRANK, D. D., MANSOURIAN, S., SUH, G. S., GALLIO, M. & STENSMYR, M.
1027 C. 2016. Humidity Sensing in Drosophila. *Curr Biol,* 26**,** 1352-8.
1028 FADEL, A. N., IBRAHIM, S. S., TCHOUAKUI, M., TERENCE, E., WONDJI, M. J., TCHOUPO, M., WANJI, S.
1029 & WONDJI, C. S. 2019. A combination of metabolic resistance and high frequency of the
1030 1014F kdr mutation is driving pyrethroid resistance in Anopheles coluzzii population from
1031 Guinea savanna of Cameroon. *Parasit Vectors,* 12**,** 263.
1032 GIMONNEAU, G., BOUYER, J., MORAND, S., BESANSKY, N. J., DIABATE, A. & SIMARD, F. 2010. A
1033 behavioral mechanism underlying ecological divergence in the malaria mosquito Anopheles
1034 gambiae. *Behav Ecol,* 21**,** 1087-1092.
1035 GRAU-BOVE, X., LUCAS, E., PIPINI, D., RIPPON, E., VAN 'T HOF, A. E., CONSTANT, E., DADZIE, S.,
1036 EGYIR-YAWSON, A., ESSANDOH, J., CHABI, J., DJOGBENOU, L., HARDING, N. J., MILES, A.,
1037 KWIATKOWSKI, D., DONNELLY, M. J., WEETMAN, D. & ANOPHELES GAMBIAE GENOMES, C.
1038 2021. Resistance to pirimiphos-methyl in West African Anopheles is spreading via
1039 duplication and introgression of the Ace1 locus. *PLoS Genet,* 17**,** e1009253.
1040 GREPPI, C., LAURSEN, W. J., BUDELLI, G., CHANG, E. C., DANIELS, A. M., VAN GIESEN, L., SMIDLER, A.
1041 L., CATTERUCCIA, F. & GARRITY, P. A. 2020. Mosquito heat seeking is driven by an ancestral
1042 cooling receptor. *Science,* 367**,** 681-684.
1043 GU, Z., EILS, R. & SCHLESNER, M. 2016. Complex heatmaps reveal patterns and correlations in
1044 multidimensional genomic data. *Bioinformatics,* 32**,** 2847-9.
1045 HALL, T. A. BioEdit: a user-friendly biological sequence alignment editor and analysis program for
1046 Windows 95/98/NT. Nucleic acids symposium series, 1999. 95-98.
1047 HU, H. X., ZHOU, D., MA, L., SHEN, B., SUN, Y. & ZHU, C. L. 2020. Lipase is associated with
1048 deltamethrin resistance in Culex pipiens pallens. *Parasitol Res,* 119**,** 23-30.
1049 HUDSON, R. R., SLATKIN, M. & MADDISON, W. P. 1992. Estimation of levels of gene flow from DNA
1050 sequence data. *Genetics,* 132**,** 583-9.

1051 HUESTIS, D. L., ARTIS, M. L., ARMBRUSTER, P. A. & LEHMANN, T. 2017. Photoperiodic responses of
1052 Sahelian malaria mosquitoes Anopheles coluzzii and An. arabiensis. *Parasit Vectors,* 10**,** 621.
1053 IBRAHIM, S. S., FADEL, A. N., TCHOUAKUI, M., TERENCE, E., WONDJI, M. J., TCHOUPO, M., KERAH-
1054 HINZOUMBE, C., WANJI, S. & WONDJI, C. S. 2019a. High insecticide resistance in the major
1055 malaria vector Anopheles coluzzii in Chad Republic. *Infect Dis Poverty,* 8**,** 100.
1056 IBRAHIM, S. S., MUKHTAR, M. M., DATTI, J. A., IRVING, H., KUSIMO, M. O., TCHAPGA, W., LAWAL, N.,
1057 SAMBO, F. I. & WONDJI, C. S. 2019b. Temporal escalation of Pyrethroid Resistance in the
1058 major malaria vector Anopheles coluzzii from Sahelo-Sudanian Region of northern Nigeria.
1059 *Scientific reports,* 9**,** 7395.
1060 IBRAHIM, S. S., MUKHTAR, M. M., IRVING, H., LABBO, R., KUSIMO, M. O., MAHAMADOU, I. &
1061 WONDJI, C. S. 2019c. High Plasmodium infection and multiple insecticide resistance in a
1062 major malaria vector Anopheles coluzzii from Sahel of Niger Republic. *Malaria journal,* 18**,**
1063 181.
1064 IBRAHIM, S. S., MUKHTAR, M. M., MUHAMMAD, A. & WONDJI, C. S. 2021. 2La Paracentric
1065 Chromosomal Inversion and Overexpressed Metabolic Genes Enhance Thermotolerance and
1066 Pyrethroid Resistance in the Major Malaria Vector Anopheles gambiae. *Biology (Basel),* 10.
1067 IBRAHIM, S. S., RIVERON, J. M., BIBBY, J., IRVING, H., YUNTA, C., PAINE, M. J. I. & WONDJI, C. S. 2015.
1068 Allelic Variation of Cytochrome P450s Drives Resistance to Bednet Insecticides in a Major
1069 Malaria Vector. *PLoS Genet,* 11**,** e1005618.
1070 JOSHI, N. & FASS, J. 2011. Sickle: A sliding-window, adaptive, quality-based trimming tool for FastQ
1071 files (Version 1.33)[Software].
1072 KEFI, M., CHARAMIS, J., BALABANIDOU, V., IOANNIDIS, P., RANSON, H., INGHAM, V. A. & VONTAS, J.
1073 2021. Transcriptomic analysis of resistance and short-term induction response to
1074 pyrethroids, in Anopheles coluzzii legs. *BMC Genomics,* 22**,** 891.
1075 KUMAR, S., STECHER, G., LI, M., KNYAZ, C. & TAMURA, K. 2018. MEGA X: Molecular Evolutionary
1076 Genetics Analysis across Computing Platforms. *Mol Biol Evol,* 35**,** 1547-1549.
1077 LEES, R. S., ISMAIL, H. M., LOGAN, R. A. E., MALONE, D., DAVIES, R., ANTHOUSI, A., ADOLFI, A.,
1078 LYCETT, G. J. & PAINE, M. J. I. 2020. New insecticide screening platforms indicate that
1079 Mitochondrial Complex I inhibitors are susceptible to cross-resistance by mosquito P450s
1080 that metabolise pyrethroids. *Sci Rep,* 10**,** 16232.
1081 LEHMANN, T., WEETMAN, D., HUESTIS, D. L., YARO, A. S., KASSOGUE, Y., DIALLO, M., DONNELLY, M.
1082 J. & DAO, A. 2017. Tracing the origin of the early wet-season Anopheles coluzzii in the Sahel.
1083 *Evol Appl,* 10**,** 704-717.
1084 LINDSAY, S., PARSON, L. AND THOMAS, C. 1998. Mapping the range and relative abundance of the
1085 two principal African malaria vectors, Anopheles gambiae sensu stricto and An. arabiensis,
1086 using climate data. *Proceedings of the Royal Society of London B: Biological Science,* 265**,**
1087 847–854.
1088 LOVE, M. I., HUBER, W., & ANDERS, S. 2014. Moderated estimation of fold change and dispersion for
1089 RNA-seq data with DESeq2. *Genome Biology,* 15.
1090 LOVE, R. R., REDMOND, S. N., POMBI, M., CAPUTO, B., PETRARCA, V., DELLA TORRE, A., ANOPHELES
1091 GAMBIAE GENOMES, C. & BESANSKY, N. J. 2019. In Silico Karyotyping of Chromosomally
1092 Polymorphic Malaria Mosquitoes in the Anopheles gambiae Complex. *G3 (Bethesda),* 9**,**
1093 3249-3262.
1094 LUCAS, E. R., ROCKETT, K. A., LYND, A., ESSANDOH, J., GRISALES, N., KEMEI, B., NJOROGE, H.,
1095 HUBBART, C., RIPPON, E. J., MORGAN, J., VAN'T HOF, A. E., OCHOMO, E. O., KWIATKOWSKI,
1096 D. P., WEETMAN, D. & DONNELLY, M. J. 2019. A high throughput multi-locus insecticide
1097 resistance marker panel for tracking resistance emergence and spread in Anopheles
1098 gambiae. *Sci Rep,* 9**,** 13335.
1099 LYND, A. & LYCETT, G. J. 2011. Optimization of the Gal4-UAS system in an Anopheles gambiae cell
1100 line. *Insect Mol Biol,* 20**,** 599-608.

1101 MARTIN, M. 2011. Cutadapt removes adapter sequences from high-throughput sequencing reads.
1102 *EMBnet. journal,* 17**,** 10-12.
1103 MENZE, B. D., KOUAMO, M. F., WONDJI, M. J., TCHAPGA, W., TCHOUPO, M., KUSIMO, M. O.,
1104 MOUHAMADOU, C. S., RIVERON, J. M. & WONDJI, C. S. 2020. An Experimental Hut
1105 Evaluation of PBO-Based and Pyrethroid-Only Nets against the Malaria Vector Anopheles
1106 funestus Reveals a Loss of Bed Nets Efficacy Associated with GSTe2 Metabolic Resistance.
1107 *Genes (Basel),* 11.
1108 MESSENGER, L. A., IMPOINVIL, L. M., DERILUS, D., YEWHALAW, D., IRISH, S. & LENHART, A. 2021. A
1109 whole transcriptomic approach provides novel insights into the molecular basis of
1110 organophosphate and pyrethroid resistance in Anopheles arabiensis from Ethiopia. *Insect*
1111 *Biochem Mol Biol,* 139**,** 103655.
1112 MITCHELL, S. N., RIGDEN, D. J., DOWD, A. J., LU, F., WILDING, C. S., WEETMAN, D., DADZIE, S.,
1113 JENKINS, A. M., REGNA, K., BOKO, P., DJOGBENOU, L., MUSKAVITCH, M. A., RANSON, H.,
1114 PAINE, M. J., MAYANS, O. & DONNELLY, M. J. 2014. Metabolic and target-site mechanisms
1115 combine to confer strong DDT resistance in Anopheles gambiae. *PLoS One,* 9**,** e92662.
1116 MITCHELL, S. N., STEVENSON, B. J., MULLER, P., WILDING, C. S., EGYIR-YAWSON, A., FIELD, S. G.,
1117 HEMINGWAY, J., PAINE, M. J., RANSON, H. & DONNELLY, M. J. 2012a. Identification and
1118 validation of a gene causing cross-resistance between insecticide classes in Anopheles
1119 gambiae from Ghana. *Proc Natl Acad Sci U S A,* 109**,** 6147-52.
1120 MITCHELL, S. N., STEVENSON, B. J., MÜLLER, P., WILDING, C. S., EGYIR-YAWSON, A., FIELD, S. G.,
1121 HEMINGWAY, J., PAINE, M. J., RANSON, H. & DONNELLY, M. J. 2012b. Identification and
1122 validation of a gene causing cross-resistance between insecticide classes in Anopheles
1123 gambiae from Ghana. *Proceedings of the National Academy of Sciences,* 109**,** 6147-6152.
1124 MUGENZI, L. M. J., MENZE, B. D., TCHOUAKUI, M., WONDJI, M. J., IRVING, H., TCHOUPO, M., HEARN,
1125 J., WEEDALL, G. D., RIVERON, J. M. & WONDJI, C. S. 2019. Cis-regulatory CYP6P9b
1126 P450 variants associated with loss of insecticide-treated bed net efficacy against Anopheles
1127 funestus. *Nat Commun,* 10**,** 4652.
1128 MULLER, P., WARR, E., STEVENSON, B. J., PIGNATELLI, P. M., MORGAN, J. C., STEVEN, A., YAWSON, A.
1129 E., MITCHELL, S. N., RANSON, H., HEMINGWAY, J., PAINE, M. J. & DONNELLY, M. J. 2008.
1130 Field-caught permethrin-resistant Anopheles gambiae overexpress CYP6P3, a P450 that
1131 metabolises pyrethroids. *PLoS Genet,* 4**,** e1000286.
1132 RANSON, H., ABDALLAH, H., BADOLO, A., GUELBEOGO, W. M., KERAH-HINZOUMBE, C., YANGALBE-
1133 KALNONE, E., SAGNON, N., SIMARD, F. & COETZEE, M. 2009. Insecticide resistance in
1134 Anopheles gambiae: data from the first year of a multi-country study highlight the extent of
1135 the problem. *Malar J,* 8**,** 299.
1136 RIVERON, J. M., HUIJBEN, S., TCHAPGA, W., TCHOUAKUI, M., WONDJI, M. J., TCHOUPO, M., IRVING,
1137 H., CUAMBA, N., MAQUINA, M., PAAIJMANS, K. & WONDJI, C. S. 2019. Escalation of
1138 Pyrethroid Resistance in the Malaria Vector Anopheles funestus Induces a Loss of Efficacy of
1139 Piperonyl Butoxide-Based Insecticide-Treated Nets in Mozambique. *J Infect Dis,* 220**,** 467-
1140 475.
1141 RIVERON, J. M., IBRAHIM, S. S., CHANDA, E., MZILAHOWA, T., CUAMBA, N., IRVING, H., BARNES, K.
1142 G., NDULA, M. & WONDJI, C. S. 2014a. The highly polymorphic CYP6M7 cytochrome P450
1143 gene partners with the directionally selected CYP6P9a and CYP6P9b genes to expand the
1144 pyrethroid resistance front in the malaria vector Anopheles funestus in Africa. *BMC*
1145 *Genomics,* 15**,** 817.
1146 RIVERON, J. M., IBRAHIM, S. S., MULAMBA, C., DJOUAKA, R., IRVING, H., WONDJI, M. J., ISHAK, I. H.
1147 & WONDJI, C. S. 2017. Genome-Wide Transcription and Functional Analyses Reveal
1148 Heterogeneous Molecular Mechanisms Driving Pyrethroids Resistance in the Major Malaria
1149 Vector Anopheles funestus Across Africa. *G3 (Bethesda),* 7**,** 1819-1832.

1150 RIVERON, J. M., TCHOUAKUI M., MUGENZI L., MENZE B. D., MU-CHUN C. AND WONDJI C. S. 2018.
1151 Insecticide Resistance in Malaria Vectors: An Update at a Global Scale. *In:* S. MANGUIN, V. D.
1152 (ed.) *Towards Malaria Elimination - A Leap Forward.* London: IntechOpen.
1153 RIVERON, J. M., YUNTA, C., IBRAHIM, S. S., DJOUAKA, R., IRVING, H., MENZE, B. D., ISMAIL, H. M.,
1154 HEMINGWAY, J., RANSON, H., ALBERT, A. & WONDJI, C. S. 2014b. A single mutation in the
1155 GSTe2 gene allows tracking of metabolically based insecticide resistance in a major malaria
1156 vector. *Genome Biol,* 15**,** R27.
1157 ROZAS, J., FERRER-MATA, A., SANCHEZ-DELBARRIO, J. C., GUIRAO-RICO, S., LIBRADO, P., RAMOS-
1158 ONSINS, S. E. & SANCHEZ-GRACIA, A. 2017. DnaSP 6: DNA Sequence Polymorphism Analysis
1159 of Large Data Sets. *Mol Biol Evol,* 34**,** 3299-3302.
1160 SCHMITTGEN, T. D. & LIVAK, K. J. 2008. Analyzing real-time PCR data by the comparative C(T)
1161 method. *Nat Protoc,* 3**,** 1101-8.
1162 SHIFF, C. 2002. Integrated approach to malaria control. *Clin Microbiol Rev,* 15**,** 278-93.
1163 STEVENSON, B. J., BIBBY, J., PIGNATELLI, P., MUANGNOICHAROEN, S., O'NEILL, P. M., LIAN, L. Y.,
1164 MULLER, P., NIKOU, D., STEVEN, A., HEMINGWAY, J., SUTCLIFFE, M. J. & PAINE, M. J. 2011.
1165 Cytochrome P450 6M2 from the malaria vector Anopheles gambiae metabolizes
1166 pyrethroids: Sequential metabolism of deltamethrin revealed. *Insect Biochem Mol Biol,* 41**,**
1167 492-502.
1168 SUPEK, F., BOSNJAK, M., SKUNCA, N. & SMUC, T. 2011. REVIGO summarizes and visualizes long lists
1169 of gene ontology terms. *PLoS One,* 6**,** e21800.
1170 TCHOUAKUI, M., RIVERON, J. M., DJONABAYE, D., TCHAPGA, W., IRVING, H., SOH TAKAM, P.,
1171 NJIOKOU, F. & WONDJI, C. S. 2018. Fitness Costs of the Glutathione S-Transferase Epsilon 2
1172 (L119F-GSTe2) Mediated Metabolic Resistance to Insecticides in the Major African Malaria
1173 Vector Anopheles Funestus. *Genes (Basel),* 9.
1174 TOE, K. H., N'FALE, S., DABIRE, R. K., RANSON, H. & JONES, C. M. 2015. The recent escalation in
1175 strength of pyrethroid resistance in Anopheles coluzzi in West Africa is linked to increased
1176 expression of multiple gene families. *BMC Genomics,* 16**,** 146.
1177 VANHOOK, A. M. 2016. Understanding hygrosensation: How flies sense changes in humidity. *Science*
1178 *Signaling,* 9**,** ec127-ec127.
1179 VANNINI, L., AUGUSTINE DUNN, W., REED, T. W. & WILLIS, J. H. 2014. Changes in transcript
1180 abundance for cuticular proteins and other genes three hours after a blood meal in
1181 Anopheles gambiae. *Insect Biochem Mol Biol,* 44**,** 33-43.
1182 VONTAS, J., GRIGORAKI, L., MORGAN, J., TSAKIRELI, D., FUSEINI, G., SEGURA, L., NIEMCZURA DE
1183 CARVALHO, J., NGUEMA, R., WEETMAN, D., SLOTMAN, M. A. & HEMINGWAY, J. 2018. Rapid
1184 selection of a pyrethroid metabolic enzyme CYP9K1 by operational malaria control activities.
1185 *Proc Natl Acad Sci U S A,* 115**,** 4619-4624.
1186 WEEDALL, G. D., MUGENZI, L. M. J., MENZE, B. D., TCHOUAKUI, M., IBRAHIM, S. S., AMVONGO-
1187 ADJIA, N., IRVING, H., WONDJI, M. J., TCHOUPO, M., DJOUAKA, R., RIVERON, J. M. &
1188 WONDJI, C. S. 2019. A cytochrome P450 allele confers pyrethroid resistance on a major
1189 African malaria vector, reducing insecticide-treated bednet efficacy. *Sci Transl Med,* 11.
1190 WEEDALL, G. D., RIVERON, J. M., HEARN, J., IRVING, H., KAMDEM, C., FOUET, C., WHITE, B. J. &
1191 WONDJI, C. S. 2020. An Africa-wide genomic evolution of insecticide resistance in the
1192 malaria vector Anopheles funestus involves selective sweeps, copy number variations, gene
1193 conversion and transposons. *PLoS Genet,* 16**,** e1008822.
1194 WEETMAN, D., WILDING, C. S., NEAFSEY, D. E., MULLER, P., OCHOMO, E., ISAACS, A. T., STEEN, K.,
1195 RIPPON, E. J., MORGAN, J. C., MAWEJJE, H. D., RIGDEN, D. J., OKEDI, L. M. & DONNELLY, M. J.
1196 2018. Candidate-gene based GWAS identifies reproducible DNA markers for metabolic
1197 pyrethroid resistance from standing genetic variation in East African Anopheles gambiae. *Sci*
1198 *Rep,* 8**,** 2920.

1199 WEILL, M., MALCOLM, C., CHANDRE, F., MOGENSEN, K., BERTHOMIEU, A., MARQUINE, M. &
1200 RAYMOND, M. 2004. The unique mutation in ace-1 giving high insecticide resistance is easily
1201 detectable in mosquito vectors. *Insect Mol Biol,* 13**,** 1-7.
1202 WHO 2015. Global Technical Strategy for Malaria 2016-2030. World Health Organisation. . Geneva,
1203 Switzerland.
1204 WHO 2018a. Update on the E-2020 initiative of 21 malaria-eliminating countries: report and country
1205 briefs. Geneva. Switzerland: World Health Organization.
1206 WHO 2018b. World Malaria Report. World Health Organization. . Geneva Switzerland.
1207 WHO 2019. World Malaria Report 2019. Geneva, Switzerland.
1208 WHO 2021. World Malaria Report. *20 years of global progress and challenges.* Geneva: Switzerland.
1209 WILLIAMS, J., COWLISHAW, R., SANOU, A., RANSON, H. & GRIGORAKI, L. 2022. In vivo functional
1210 validation of the V402L voltage gated sodium channel mutation in the malaria vector An.
1211 gambiae. *Pest Manag Sci,* 78**,** 1155-1163.
1212 YI, X., LIANG, Y., HUERTA-SANCHEZ, E., JIN, X., CUO, Z. X., POOL, J. E., XU, X., JIANG, H.,
1213 VINCKENBOSCH, N., KORNELIUSSEN, T. S., ZHENG, H., LIU, T., HE, W., LI, K., LUO, R., NIE, X.,
1214 WU, H., ZHAO, M., CAO, H., ZOU, J., SHAN, Y., LI, S., YANG, Q., ASAN, NI, P., TIAN, G., XU, J.,
1215 LIU, X., JIANG, T., WU, R., ZHOU, G., TANG, M., QIN, J., WANG, T., FENG, S., LI, G., HUASANG,
1216 LUOSANG, J., WANG, W., CHEN, F., WANG, Y., ZHENG, X., LI, Z., BIANBA, Z., YANG, G., WANG,
1217 X., TANG, S., GAO, G., CHEN, Y., LUO, Z., GUSANG, L., CAO, Z., ZHANG, Q., OUYANG, W., REN,
1218 X., LIANG, H., ZHENG, H., HUANG, Y., LI, J., BOLUND, L., KRISTIANSEN, K., LI, Y., ZHANG, Y.,
1219 ZHANG, X., LI, R., LI, S., YANG, H., NIELSEN, R., WANG, J. & WANG, J. 2010. Sequencing of 50
1220 human exomes reveals adaptation to high altitude. *Science,* 329**,** 75-8.
1221 YUNTA, C., GRISALES, N., NASZ, S., HEMMINGS, K., PIGNATELLI, P., VOICE, M., RANSON, H. & PAINE,
1222 M. J. 2016. Pyriproxyfen is metabolized by P450s associated with pyrethroid resistance in An.
1223 gambiae. *Insect Biochem Mol Biol,* 78**,** 50-57.
1224 YUNTA, C., HEMMINGS, K., STEVENSON, B., KOEKEMOER, L. L., MATAMBO, T., PIGNATELLI, P., VOICE,
1225 M., NASZ, S. & PAINE, M. J. I. 2019. Cross-resistance profiles of malaria mosquito P450s
1226 associated with pyrethroid resistance against WHO insecticides. *Pestic Biochem Physiol,* 161**,**
1227 61-67.
1228 ZHAO, L. A. J., W.A. 2012. Expression of heat shock protein genes in insect stress responses. .
1229 *Invertebrate Survival Journal,* 9**,** 93-101.

1230

1231 Figure Legends

1232 **Figure 1: A volcano plot of differentially expressed genes showing fold changes and**
1233 **significance in R-S, C-S and R-C comparisons, for Nigeria and Niger populations of *An.***
1234 ***coluzzii*.**

1235

1236 **Figure 2: A volcano plot of differentially expressed genes showing fold changes and**
1237 **significance in R-S, C-S and R-C comparisons, for Chad and Cameroon populations of *An.***
1238 ***coluzzii*.**

1239

1240 **Figure 3: Validation of candidate resistance genes.** qRT-PCR of twelve metabolic resistance
1241 genes (R-S and C-S comparisons) from Sahel *An. coluzzii.*

1242

1243 **Figure 4: Identification of resistance variants.** A heatmap showing frequencies of the
1244 resistance variants (haplotypes) in key genes of interest.

1245

1246 **Figure 5: Characterization of 5′ regulatory element of *GSTe2*.** Results of dual-luciferase
1247 reporter assays of the promoter (intergenic region) constructs, showing progressive loss of
1248 activity following sequential deletion of the constructs.

1249

1250 **Figure 6: Validation of the role of metabolic resistance genes in insecticide resistance.**
1251 Results of insecticide susceptibility bioassays with transgenic flies expressing *GSTe2* and
1252 *CYP6Z2*. **a.** α-cypermethrin and deltamethrin, b. permethrin, **c.** 3-phenoxybenzaldehyde and
1253 3-phenoxybenzyl alcohol, **d.** DDT and clothianidin.

1254

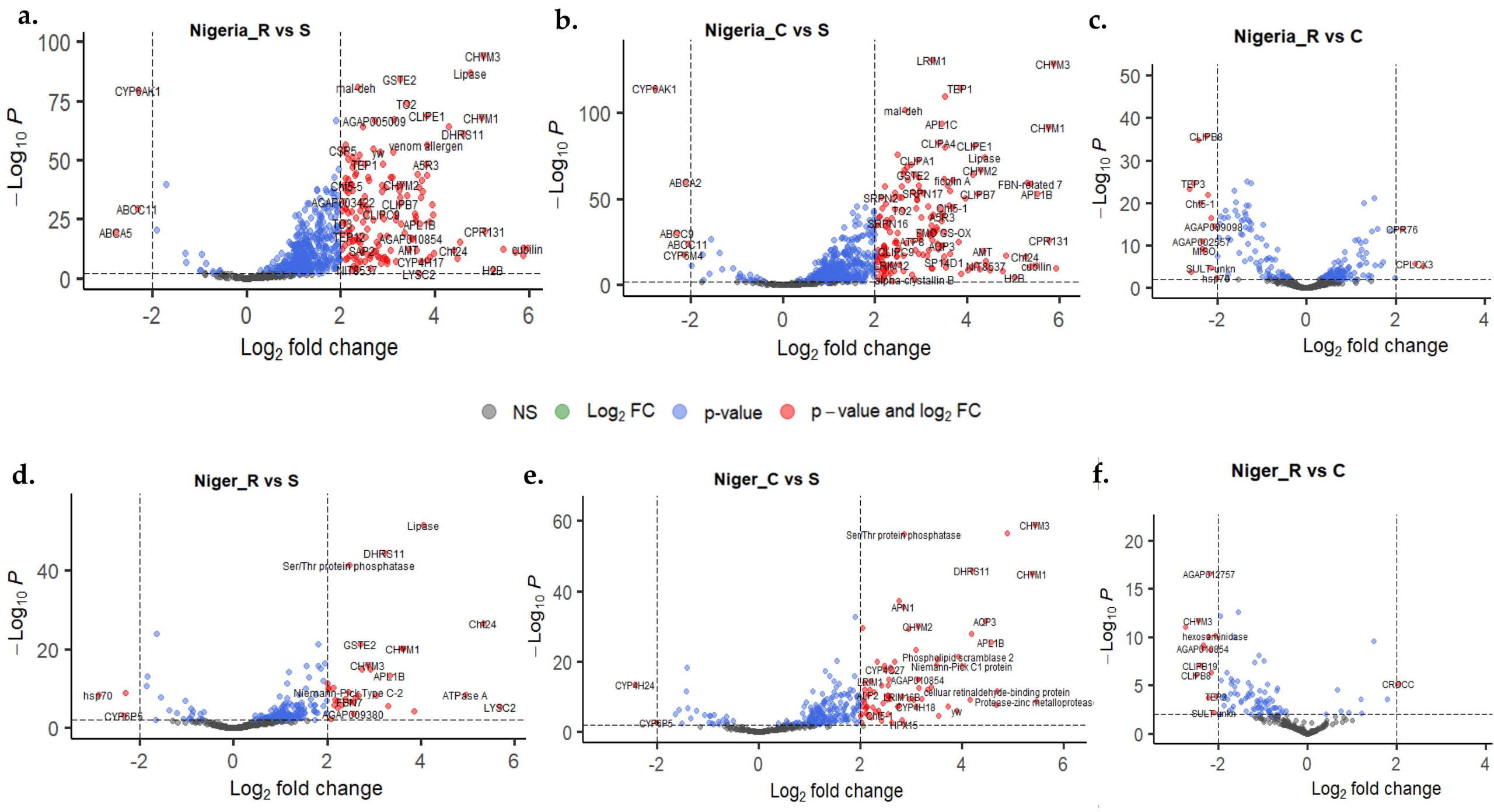
a.
Nigeria_R vs S
b.
Nigeria_C vs S
c.
Nigeria_R vs C
d.
Niger_R vs S
e.
Niger_C vs S
f.
Niger_R vs C
−Log10 P
Log2 fold change
NS
Log2 FC
p-value
p – value and log2 FC

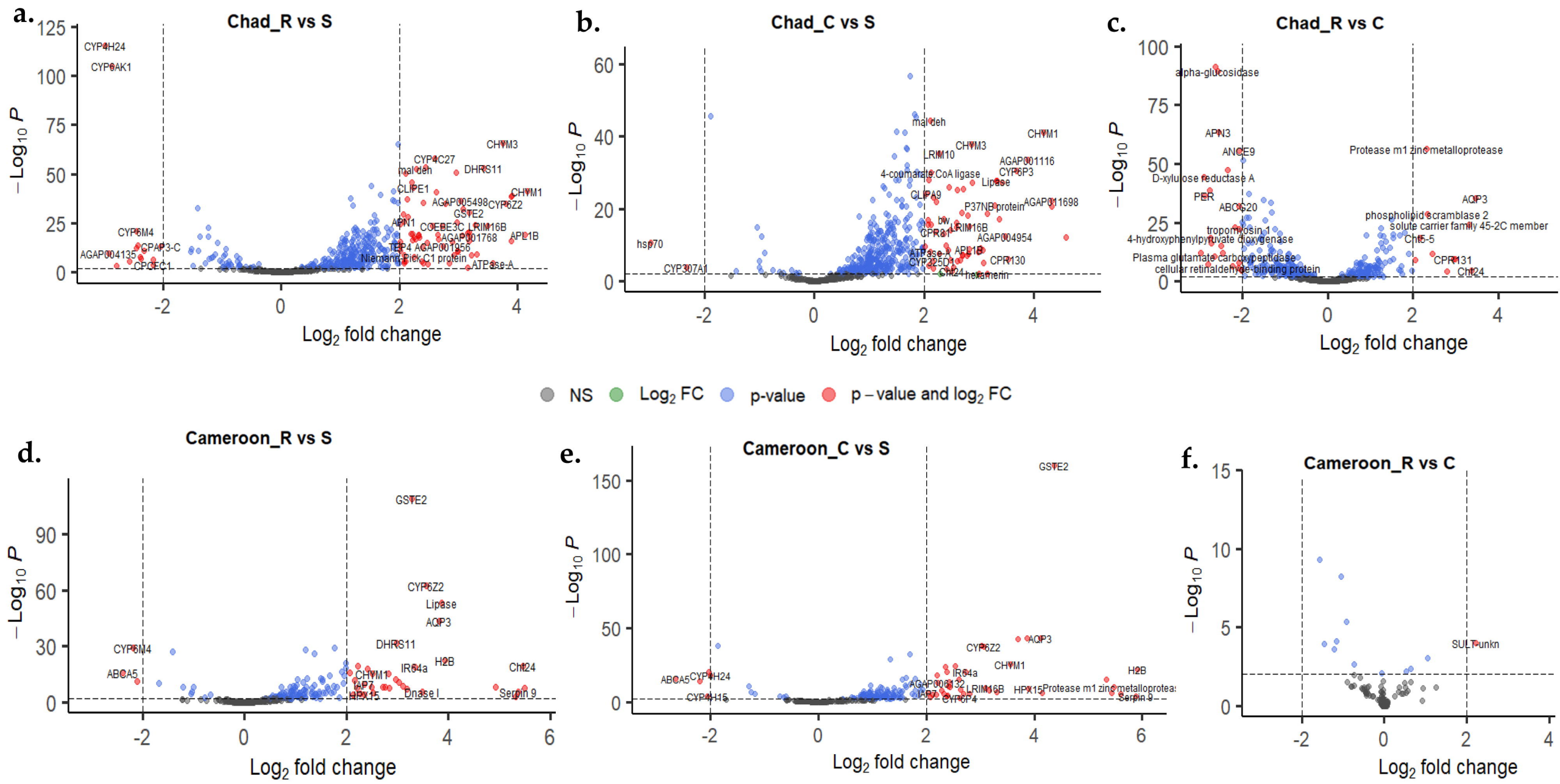
a.
Chad_R vs S
b.
Chad_C vs S
c.
Chad_R vs C
d.
Cameroon_R vs S
e.
Cameroon_C vs S
f.
Cameroon_R vs C
−Log10 P
Log2 fold change
NS
Log2 FC
p-value
p – value and log2 FC

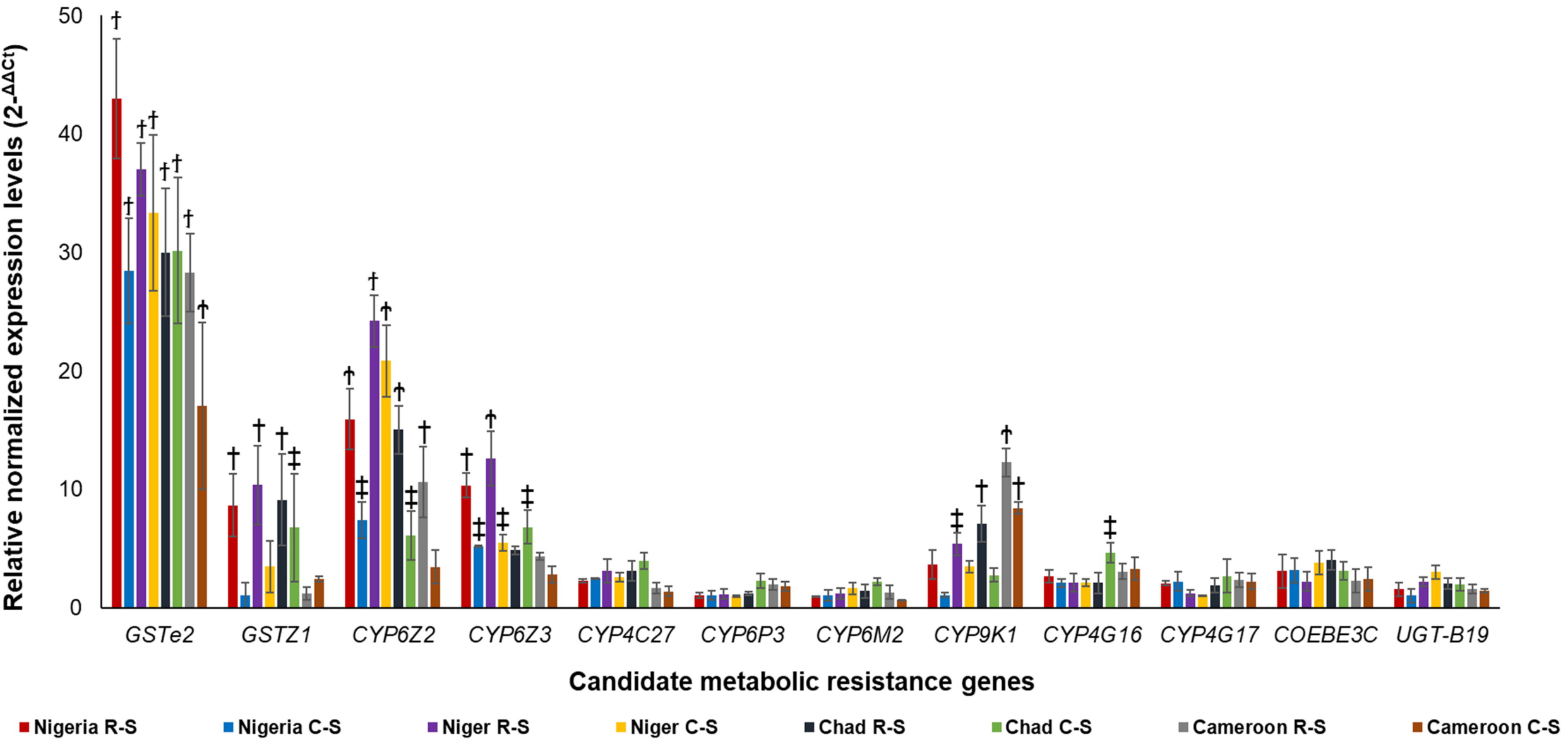
Relative normalized expression levels ($2^{-\Delta\Delta Ct}$)
50
40
30
20
10
0
GSTe2
GSTZ1
CYP6Z2
CYP6Z3
CYP4C27
CYP6P3
CYP6M2
CYP9K1
CYP4G16
CYP4G17
COEBE3C
UGT-B19
Candidate metabolic resistance genes
Nigeria R-S
Nigeria C-S
Niger R-S
Niger C-S
Chad R-S
Chad C-S
Cameroon R-S
Cameroon C-S

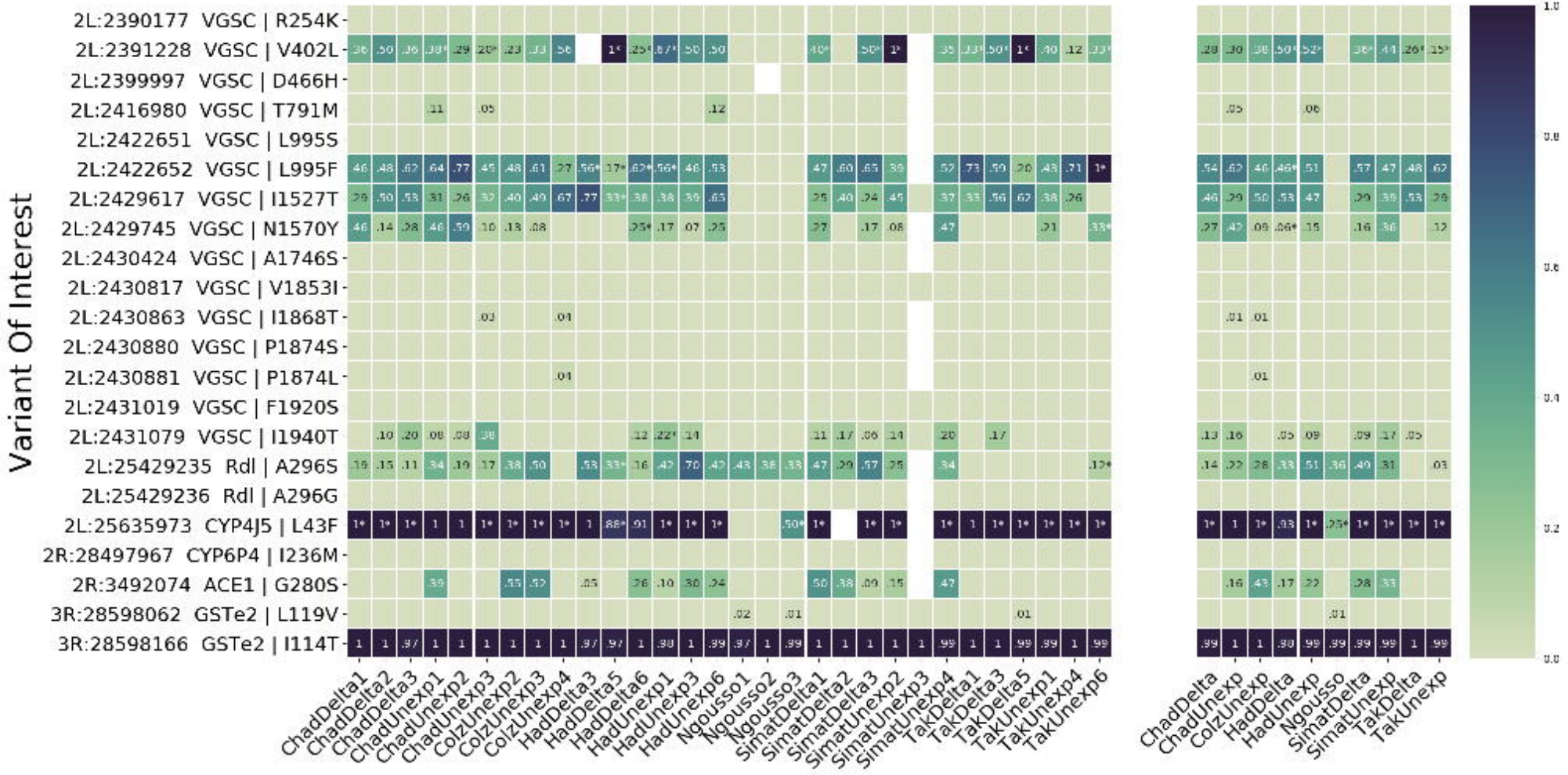
Variant Of Interest
2L:2390177 VGSC | R254K
2L:2391228 VGSC | V402L
2L:2399997 VGSC | D466H
2L:2416980 VGSC | T791M
2L:2422651 VGSC | L995S
2L:2422652 VGSC | L995F
2L:2429617 VGSC | I1527T
2L:2429745 VGSC | N1570Y
2L:2430424 VGSC | A1746S
2L:2430817 VGSC | V1853I
2L:2430863 VGSC | I1868T
2L:2430880 VGSC | P1874S
2L:2430881 VGSC | P1874L
2L:2431019 VGSC | F1920S
2L:2431079 VGSC | I1940T
2L:25429235 Rdl | A296S
2L:25429236 Rdl | A296G
2L:25635973 CYP4J5 | L43F
2R:28497967 CYP6P4 | I236M
2R:3492074 ACE1 | G280S
3R:28598062 GSTe2 | L119V
3R:28598166 GSTe2 | I114T
ChadDelta1
ChadDelta2
ChadDelta3
ChadUnexp1
ChadUnexp2
ChadUnexp3
ColzUnexp2
ColzUnexp3
ColzUnexp4
HadDelta3
HadDelta5
HadDelta6
HadUnexp1
HadUnexp3
HadUnexp6
Ngousso1
Ngousso2
Ngousso3
SimatDelta1
SimatDelta2
SimatDelta3
SimatUnexp2
SimatUnexp3
SimatUnexp4
TakDelta1
TakDelta3
TakDelta5
TakUnexp1
TakUnexp4
TakUnexp6
ChadDelta
ChadUnexp
ColzUnexp
HadDelta
HadUnexp
Ngousso
SimatDelta
SimatUnexp
TakDelta
TakUnexp
1.0
0.8
0.6
0.4
0.2
0.0

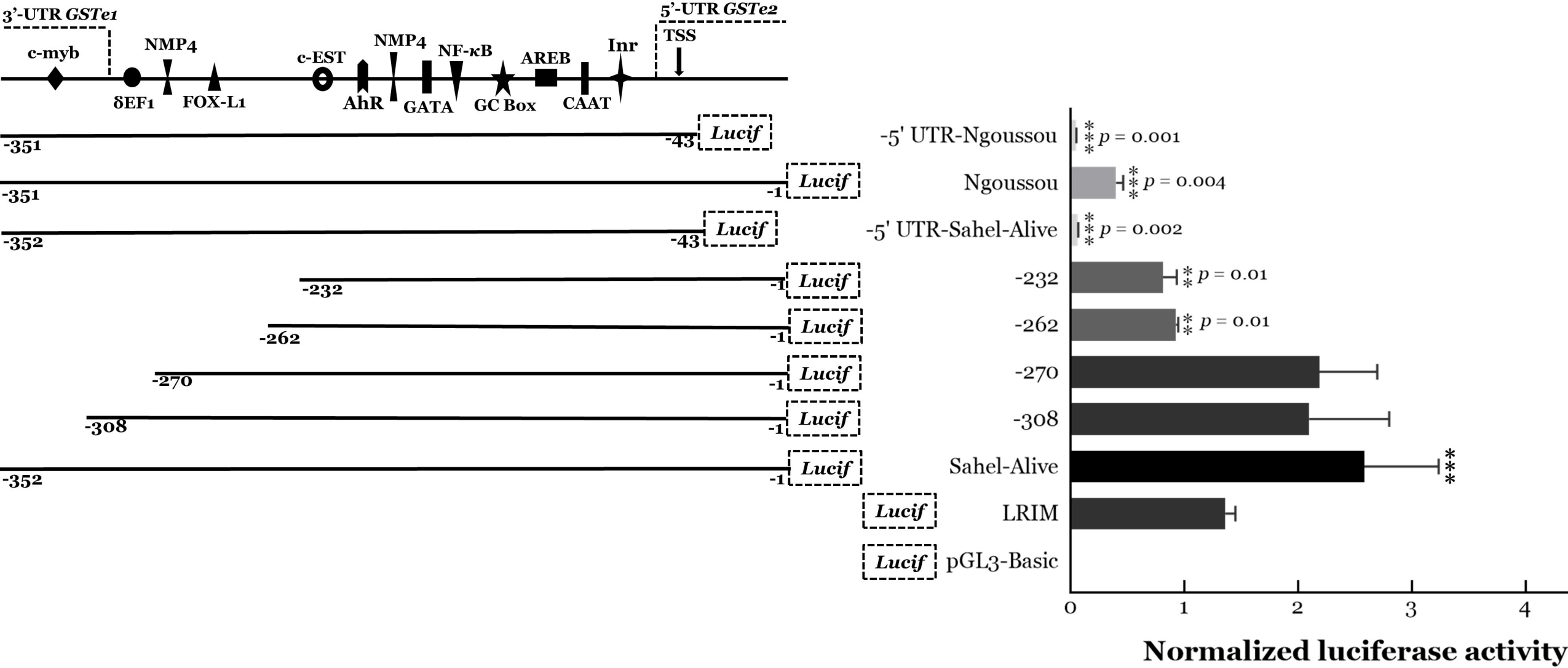
3'-UTR GSTe1
5'-UTR GSTe2
c-myb
NMP4
c-EST
NMP4
NF-κB
AREB
Inr
TSS
δEF1
FOX-L1
AhR
GATA
GC Box
CAAT
-351
-43
Lucif
-351
-1
Lucif
-352
-43
Lucif
-232
-1
Lucif
-262
-1
Lucif
-270
-1
Lucif
-308
-1
Lucif
-352
-1
Lucif
-5' UTR-Ngoussou
p = 0.001
Ngoussou
p = 0.004
-5' UTR-Sahel-Alive
p = 0.002
-232
p = 0.01
-262
p = 0.01
-270
-308
Sahel-Alive
Lucif
LRIM
Lucif
pGL3-Basic
0
1
2
3
4
Normalized luciferase activity

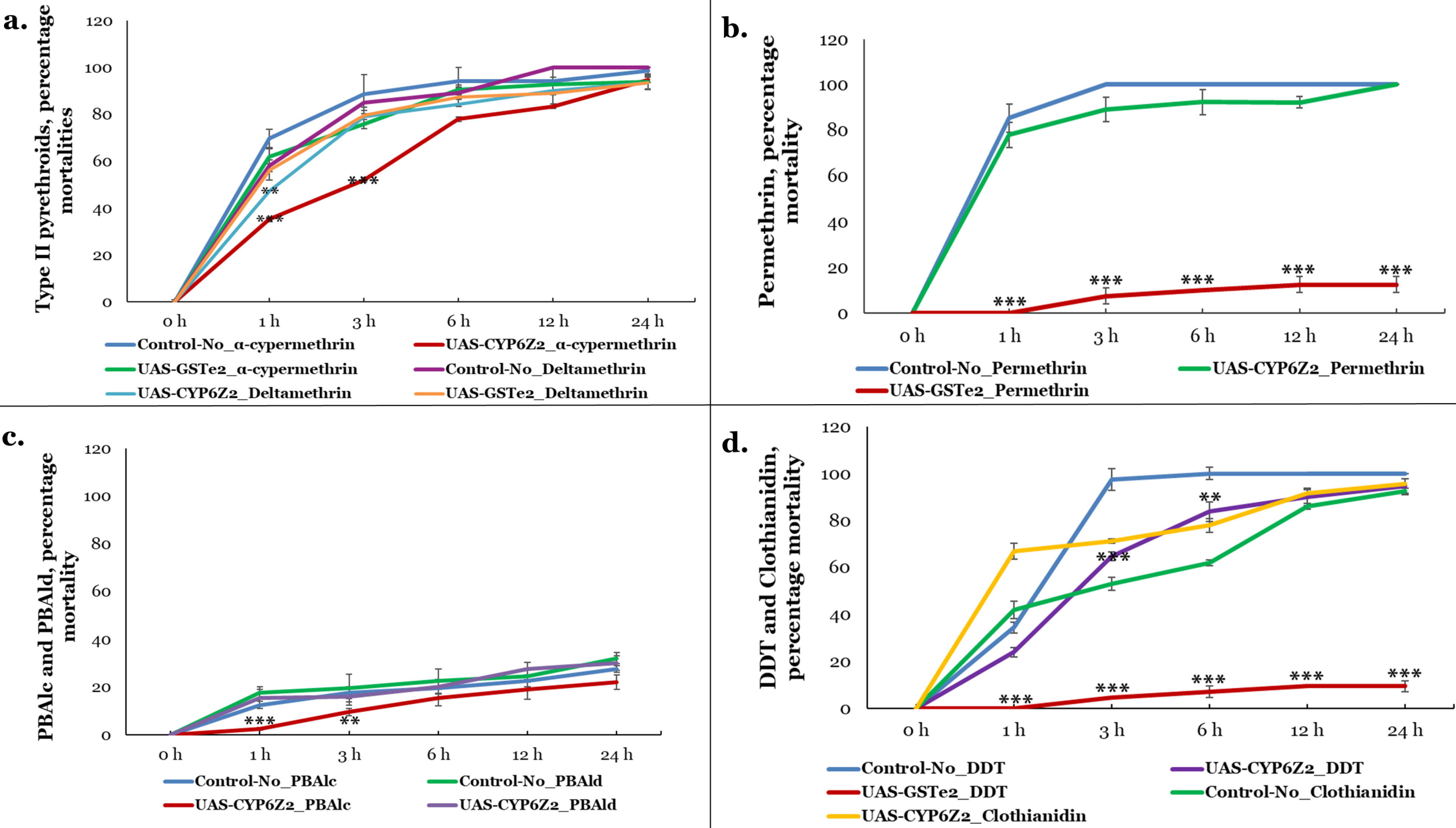
a.
Type II pyrethroids, percentage mortalities
120
100
80
60
40
20
0
0 h
1 h
3 h
6 h
12 h
24 h
**
***
***
Control-No_α-cypermethrin
UAS-CYP6Z2_α-cypermethrin
UAS-GSTe2_α-cypermethrin
Control-No_Deltamethrin
UAS-CYP6Z2_Deltamethrin
UAS-GSTe2_Deltamethrin
b.
Permethrin, percentage mortality
120
100
80
60
40
20
0
0 h
1 h
3 h
6 h
12 h
24 h
***
***
***
***
***
Control-No_Permethrin
UAS-CYP6Z2_Permethrin
UAS-GSTe2_Permethrin
c.
PBAlc and PBAld, percentage mortality
120
100
80
60
40
20
0
0 h
1 h
3 h
6 h
12 h
24 h
***
**
Control-No_PBAlc
Control-No_PBAld
UAS-CYP6Z2_PBAlc
UAS-CYP6Z2_PBAld
d.
DDT and Clothianidin, percentage mortality
120
100
80
60
40
20
0
0 h
1 h
3 h
6 h
12 h
24 h
**
***
***
***
***
***
***
Control-No_DDT
UAS-CYP6Z2_DDT
UAS-GSTe2_DDT
Control-No_Clothianidin
UAS-CYP6Z2_Clothianidin